Université de Liège
Faculté des Sciences
Département de Géologie
Laboratoire de Minéralogie

Iron-manganese phosphates with the olivine- and alluaudite-type structures: Geological applications and development of new materials

Frédéric Hatert

Halle, January 17th, 2011

- Contents

Occurrence

Université de Liège

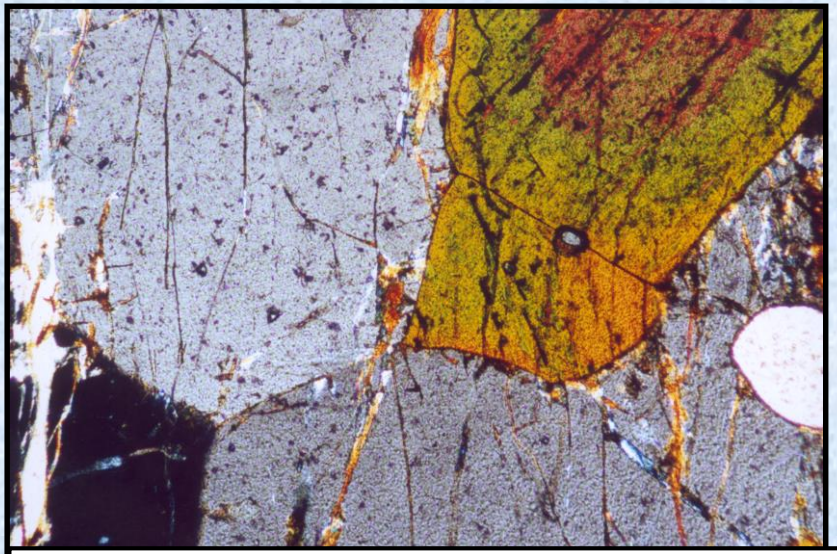

Fillowite + alluaudite, Kabira pegmatite, Uganda

- Granitic pegmatites
- Metamorphic rocks
- Meteorites

Johnsomervilleite, Loch Quoich, Scotland

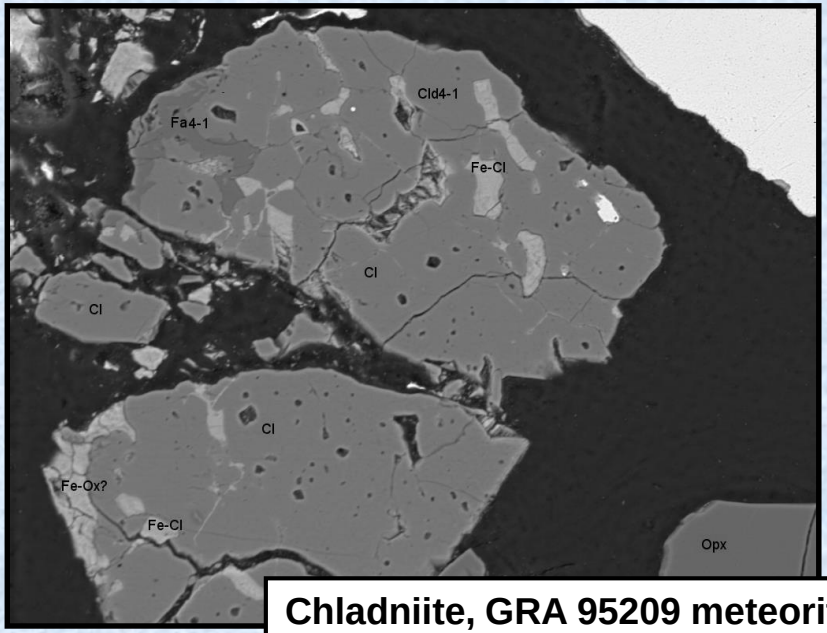

Chladniite, GRA 95209 meteorite

Fe-Mn phosphates in pegmatites

Université de Liège

Buranga pegmatite, Rwanda

Sapucaia pegmatite, Brazil

Phosphates with the olivine structure: the « Quensel-Mason » sequence

Université de Liège

$Li(Mn^{2+},Fe^{2+})PO_4 \Rightarrow {}_{x}^{\bullet}Li_{1-x}(Mn^{2+},Fe^{3+})PO_4 \Rightarrow (Mn^{3+},Fe^{3+})PO_4$
(Lithiophilite) (Sicklerite) (Purpurite)

$Li(Fe^{2+},Mn^{2+})PO_4 \Rightarrow {}_{x}^{\bullet}Li_{1-x}(Fe^{3+},Mn^{2+})PO_4 \Rightarrow (Fe^{3+},Mn^{3+})PO_4$
(Triphylite) (Ferrisicklerite) (Heterosite)

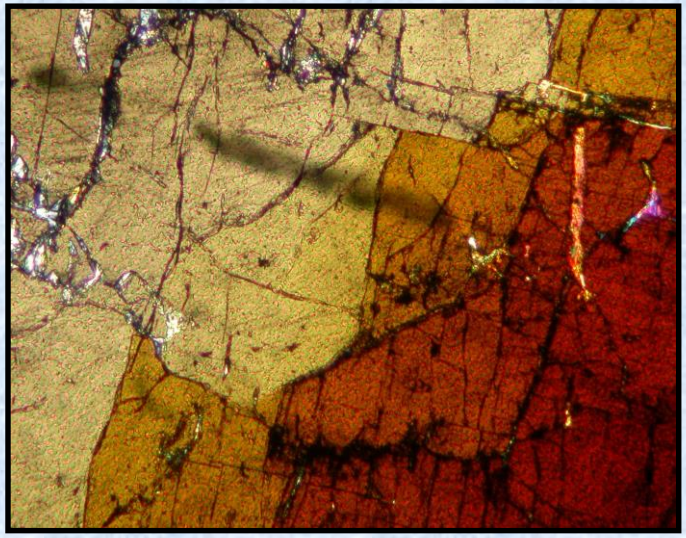

The alluaudite group of minerals

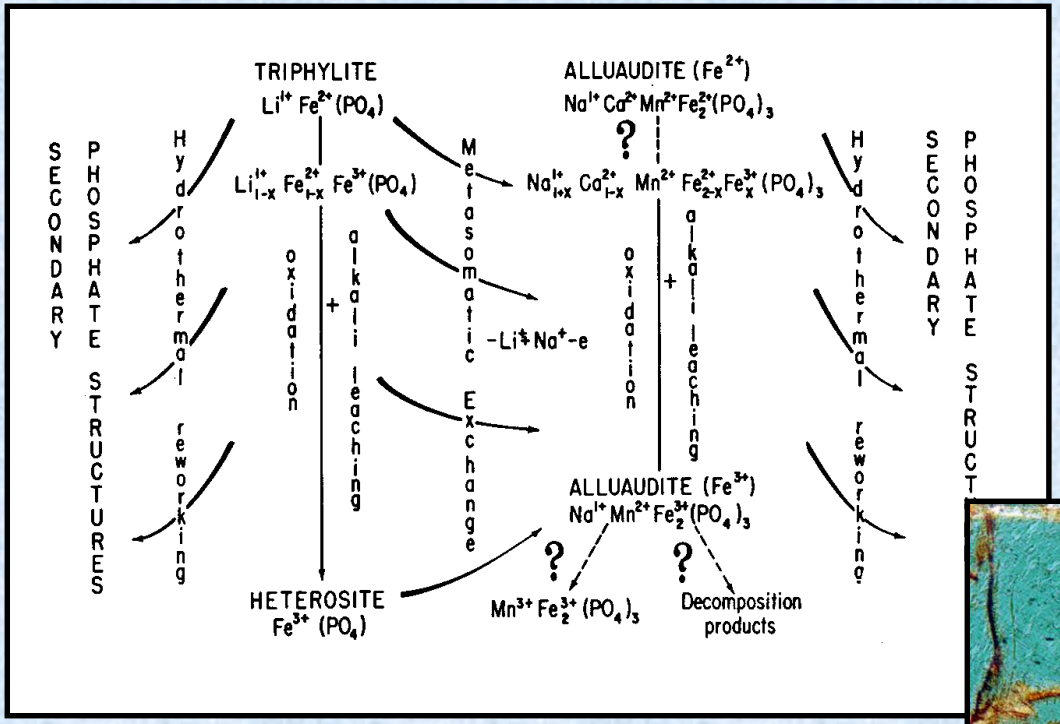

- **Secondary origin**
- **Primary origin**

Oxidation mechanism

$$Na_2MnFe^{2+}Fe^{3+}(PO_4)_3 \Rightarrow []NaMnFe^{3+}{}_2(PO_4)_3$$

$$Na^+ + Fe^{2+} \Rightarrow [] + Fe^{3+}$$

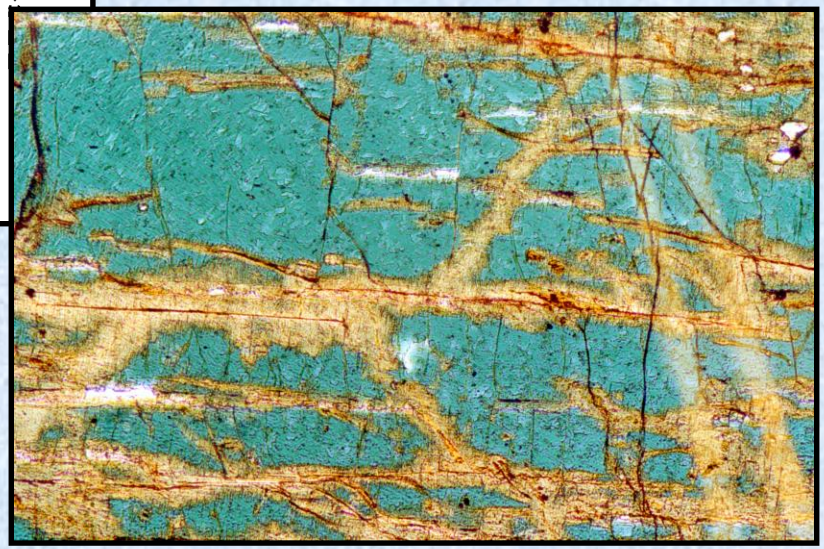

Alluaudite, Kibingo pegmatite, Rwanda

The alluaudite structure

***A*(2)'**: gable disphenoid
***A*(1)**: distorted cube
***M*(1)**: very distorted octahedron
***M*(2)**: distorted octahedron

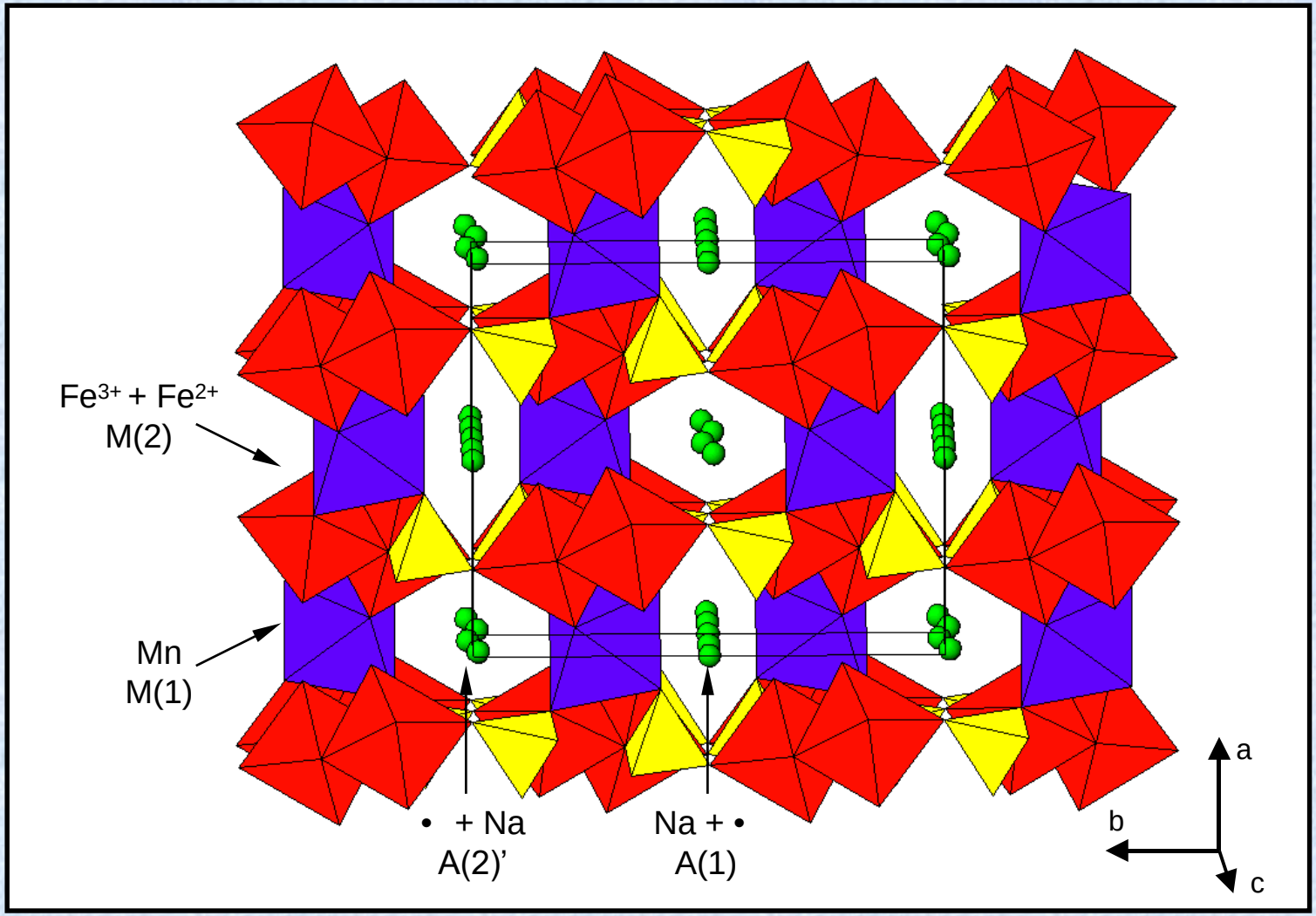

The alluaudite structure

Université de Liège

M(1)-*M*(2) chains

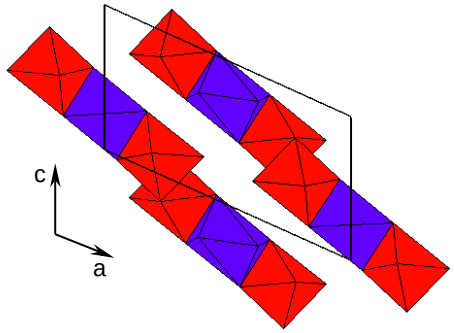

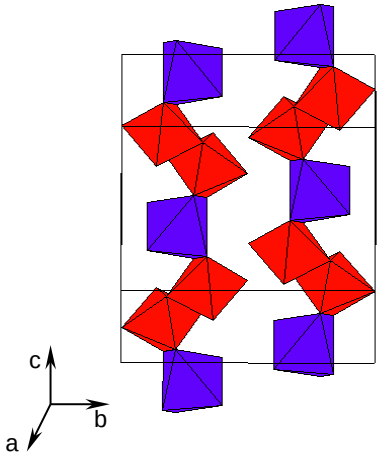

A(1) chains

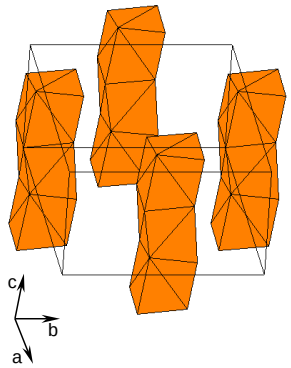

A(2)’ chains

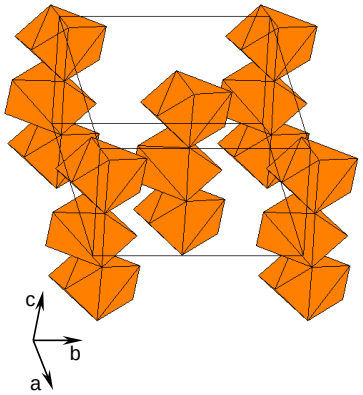

The alluaudite structural formula

- Moore (1971)

$C2/c$, $Z = 4$

$$X(2)X(1)M(1)M(2)_2(PO_4)_3$$

- Hatert *et al.* (2000)

$$[A(2)A(2)'][A(1)A(1)'A(1)''_2]M(1)M(2)_2(PO_4)_3$$

A(2), *A*(1)', *A*(1)'': generally vacant

Crystal chemistry of natural alluaudites

Université de Liège

- **Moore & Ito (1979)**

$A(2)' \Rightarrow Na^{+}, \square, K^{+}$
$A(1) \Rightarrow Na^{+}, Mn^{2+}, Ca^{2+}, \square$
$M(1) \Rightarrow Mn^{2+}, Fe^{2+}, Ca^{2+}, Mg^{2+}$
$M(2) \Rightarrow Fe^{3+}, Fe^{2+}, Mn^{2+}, Mg^{2+}, Li^{+}$

- **Fransolet *et al*. (1985, 1986, 2004)**

Oxidation mechanism:

$$Na^{+} + Fe^{2+} \Rightarrow \square + Fe^{3+}$$

$$Na_2MnFe^{2+}Fe^{3+}(PO_4)_3 \Rightarrow \square NaMnFe^{3+}{}_2(PO_4)_3$$
$$Na_2Fe^{2+}{}_2Fe^{3+}(PO_4)_3 \Rightarrow \square NaFe^{2+}Fe^{3+}{}_2(PO_4)_3$$

Crystal chemistry of synthetic alluaudite-type compounds

Université de Liège

- Solid state synthesis in air
- T = 800-950 °C
- P = 1 bar

→ $Na\text{-}Mn\text{-}Fe^{3+}$ (+ PO_4) system
→ Role of Li^+
→ Role of Cd^{2+} and Zn^{2+}
→ Role of In^{3+} and Ga^{3+}

Experimental

- Hydrothermal synthesis
- Tuttle-type cold-seal bombs
- T = 400-800 °C
- P = 1-5 kbar

→ $Na\text{-}Mn\text{-}Fe^{2+}\text{-}Fe^{3+}$ (+ PO_4) system

Cation	Ionic radius (Å) [VI]	[VIII]	Site *A*(2)'	*A*(1)	*M*(1)	*M*(2)
Ag^{+}	1.15	1.28	X	X		
Na^{+}	1.02	1.18	X	X	X	
Cu^{+}	0.77	-	p	p		
Li^{+}	0.76	0.92	p	p		
Ca^{2+}	1.00	1.12	p	p	p	
Cd^{2+}	0.95	1.10		p	X	p
Mn^{2+}	0.830	0.96	p	p	X	X
Fe^{2+}	0.780	0.92			X	X
Co^{2+}	0.745	0.90			X	X
Zn^{2+}	0.740	0.90			X	P
Cu^{2+}	0.73	-		p		
Mg^{2+}	0.720	0.89			X	X
In^{3+}	0.800	0.92			p	X
Fe^{3+}	0.645	0.78		p		X
Ga^{3+}	0.620	-				p
Cr^{3+}	0.615	-				p
Al^{3+}	0.535	-				p

X : Complete occupancy of the site
p : Partial occupancy of the site

Université de Liège

Solid-state synthesis and hydrothermal experiments

⇩

X-ray structure refinements

⇩

Cationic distribution

Université de Liège

The role of lithium in alluaudites

- $(Na_{1-x}Li_x)MnFe^{3+}_2(PO_4)_3$
  Single-crystal structure refinements
  Variations of the unit-cell parameters
  Mössbauer spectroscopy

- $(Na_{1-x}Li_x)CdIn_2(PO_4)_3$
  X-ray Rietveld refinements

- $(Na_{1-x}Li_x)_{1.5}Mn_{1.5}Fe^{3+}_{1.5}(PO_4)_3$
  X-ray Rietveld refinements

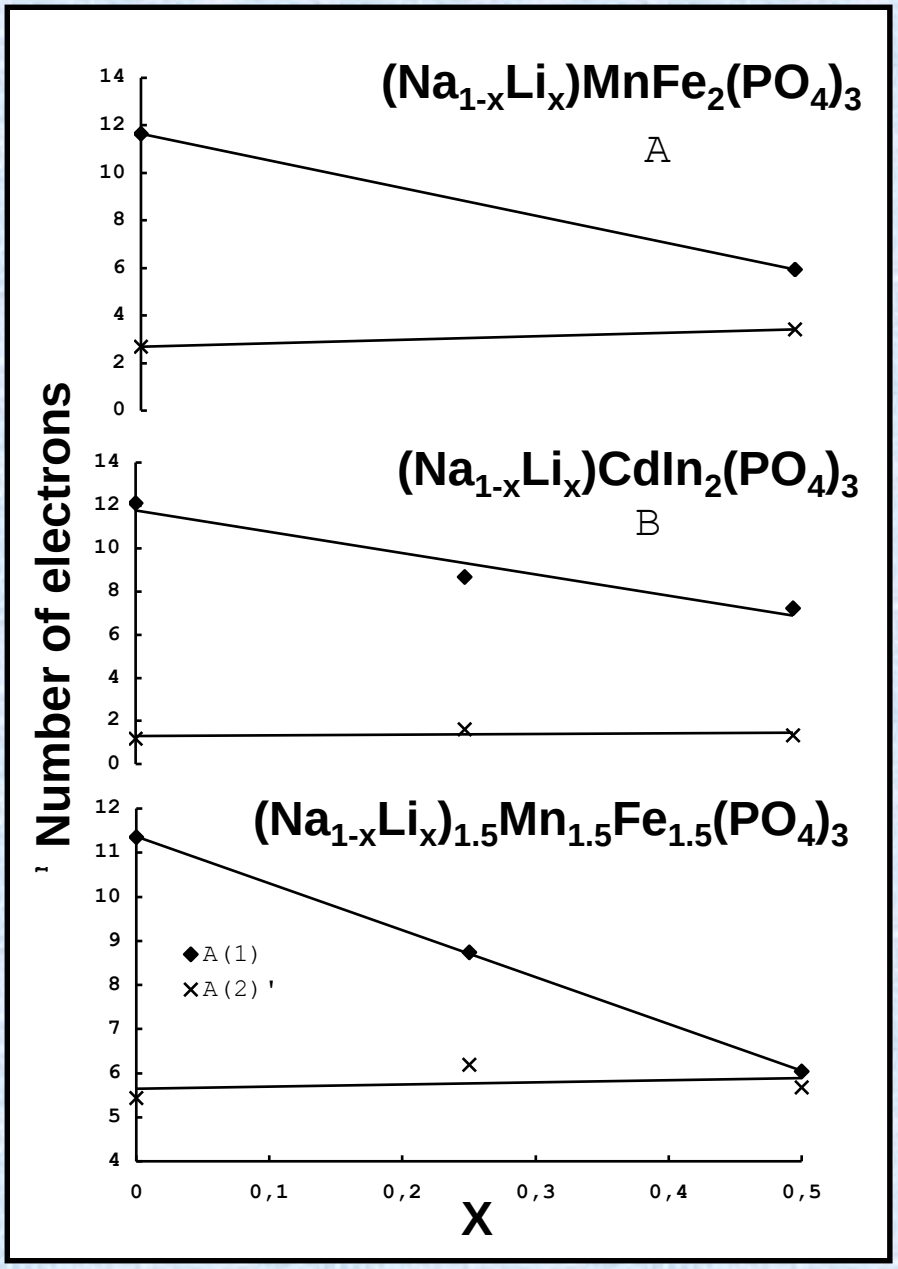

Université de Liège

Number of electrons on *A*(1) and *A*(2) ’

Li localized on the large *A*(1) site

The role of *M* cations

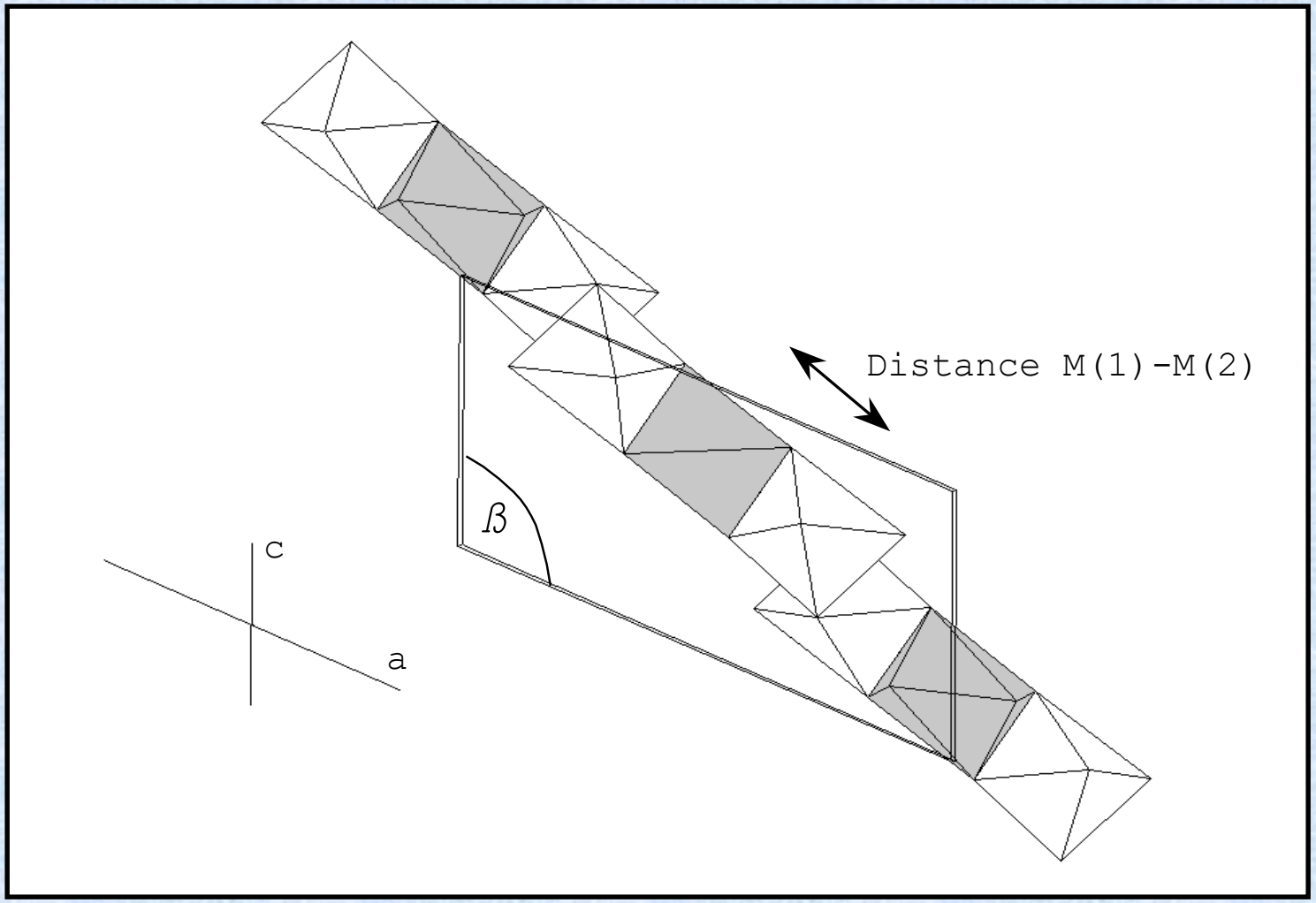

Université de Liège

$Na_{1.5}(Mn_{1-x}Zn_x)_{1.5}Fe^{3+}_{1.5}(PO_4)_3$

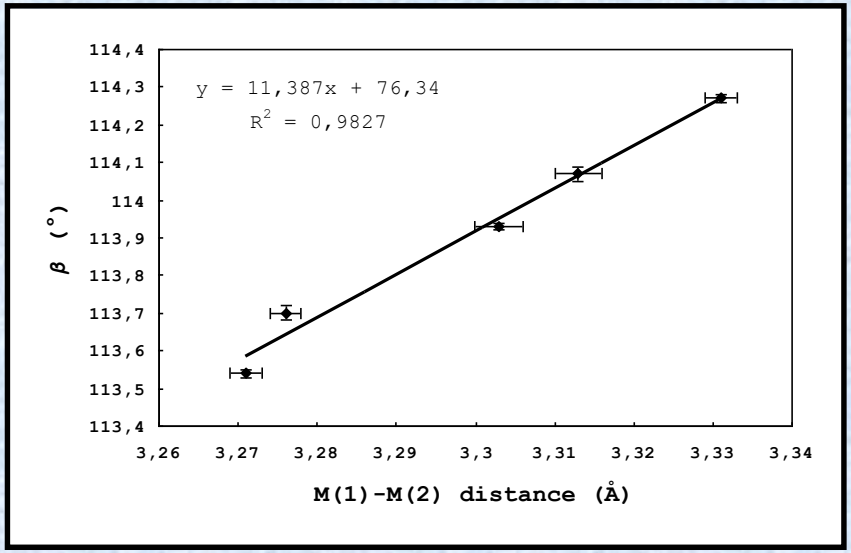

Correlations between the *M*(1)-*M*(2) distance and the beta angle

$Na_{1.5}(Mn_{1-x}Cd_x)_{1.5}Fe^{3+}_{1.5}(PO_4)_3$

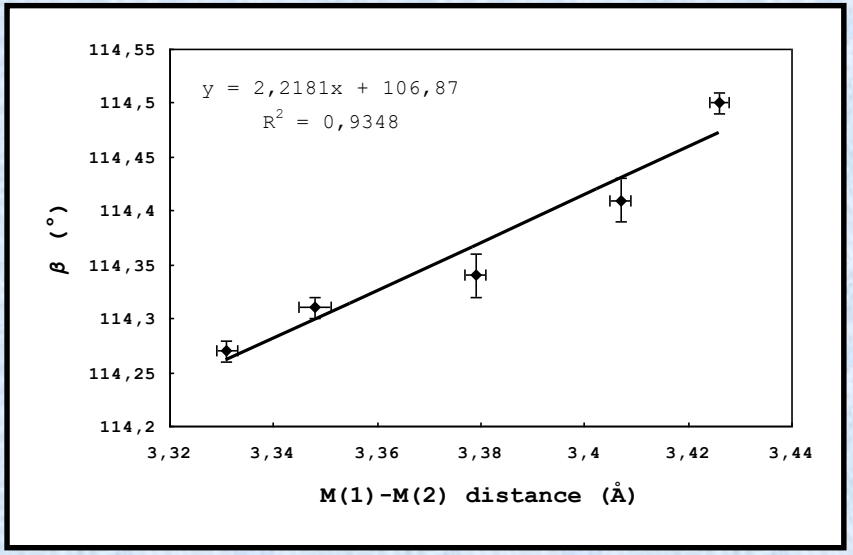

Université de Liège

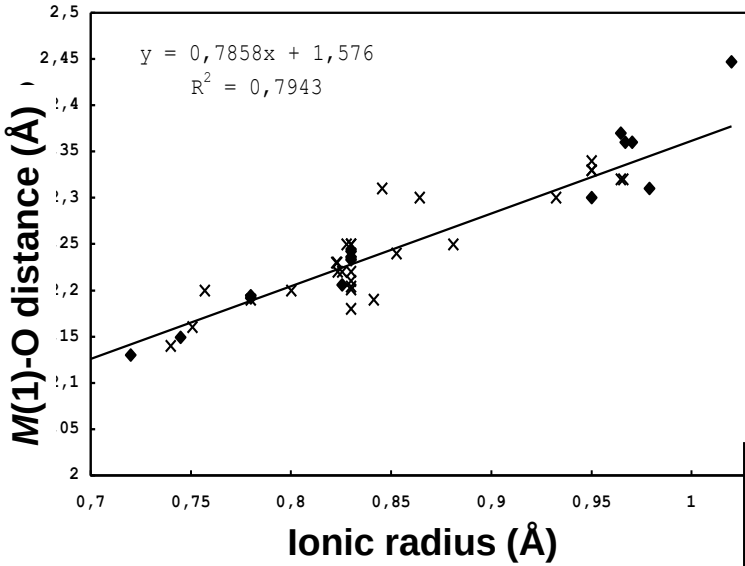

Correlations between *M*-O and the ionic radius

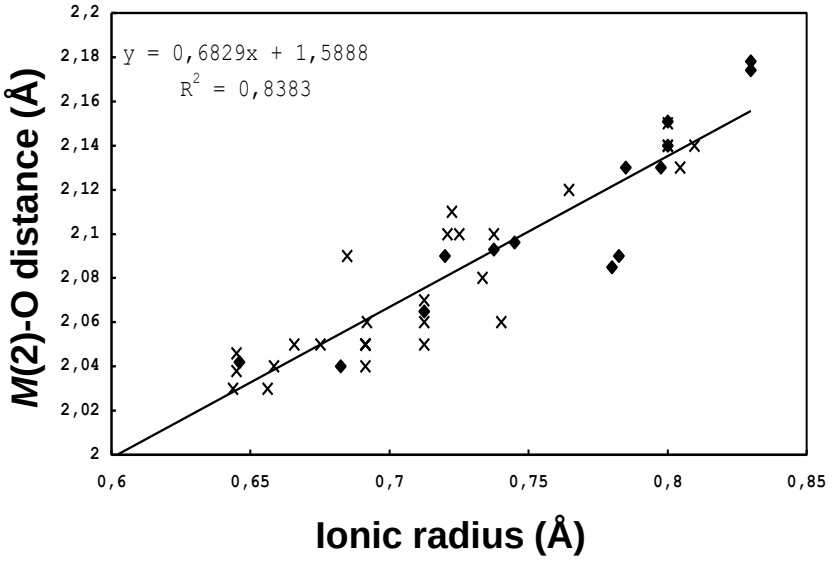

The triphylite structure

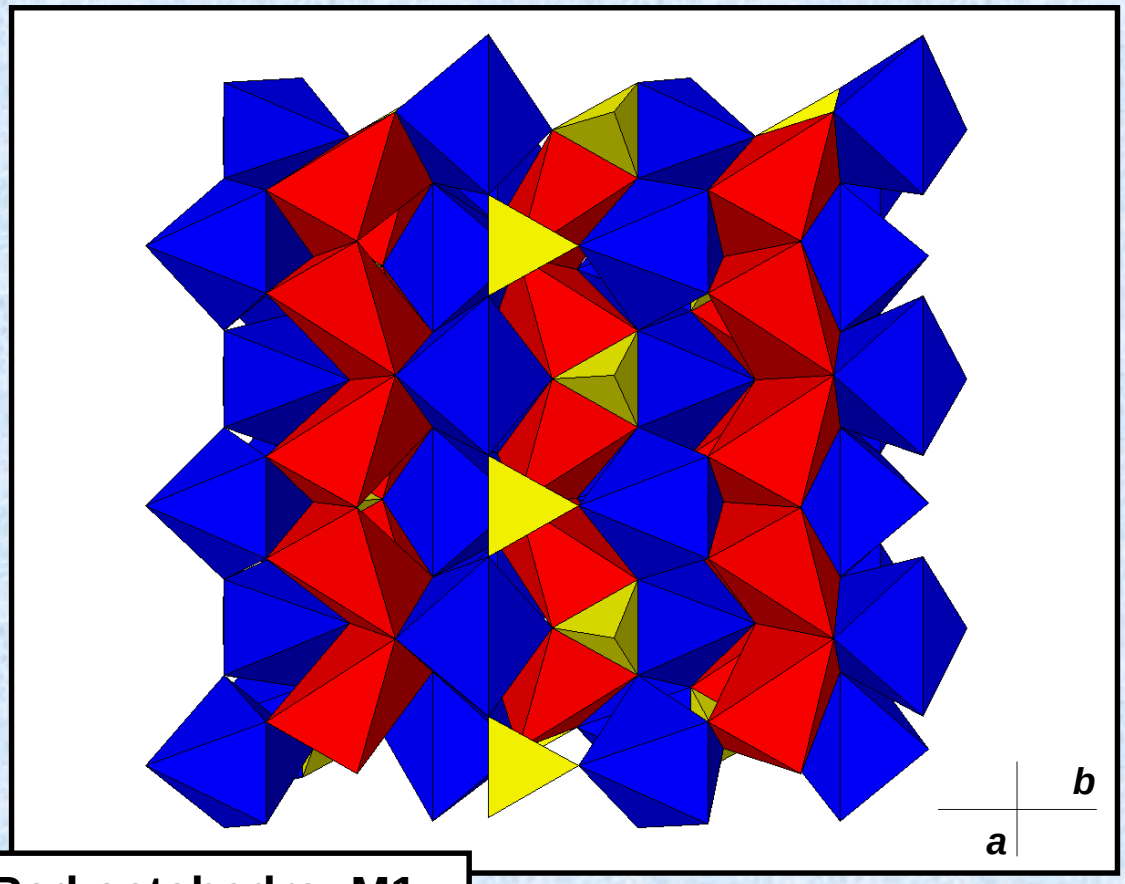

Red octahedra: M1
Blue octahedra: M2

S.G. *Pmnb*

***a* = 6.092, *b* = 10.429, *c* = 4.738 Å**

- **M1: Li, []**
- **M2: Fe^{2+}, Mn, Mg**

Crystal chemistry of natural olivine-type phosphates

Université de Liège

SIMS and crystal-structure analysis of 19 samples

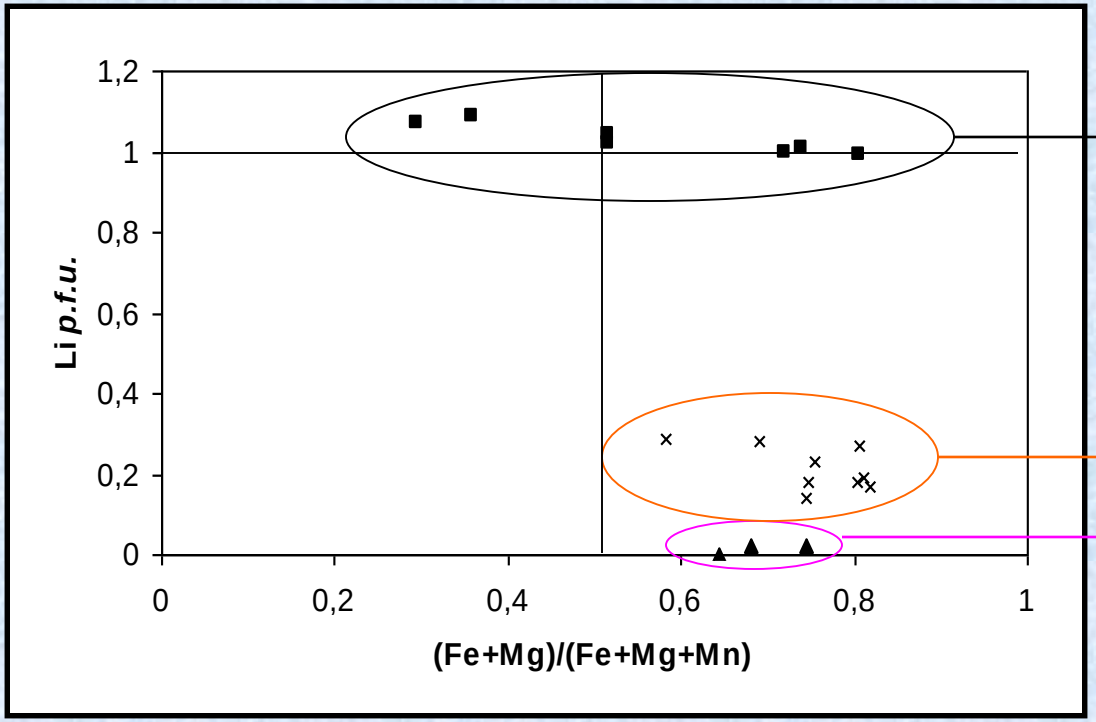

Triphylite-lithiophilite
0.99-1.07 Li *p.f.u.*

Ferrisicklerite
0.14-0.29 Li *p.f.u.*

Heterosite
0.00-0.02 Li *p.f.u.*

Heterosite may contain up to 0.21 wt. % Li_2O, and ferrisicklerite may show a low Li-content of 1.31 wt. % Li_2O

Close Li-contents!

The progressive transition from lithiophilite to sicklerite

Université de Liège

Sample from the Altaï Mountains, China

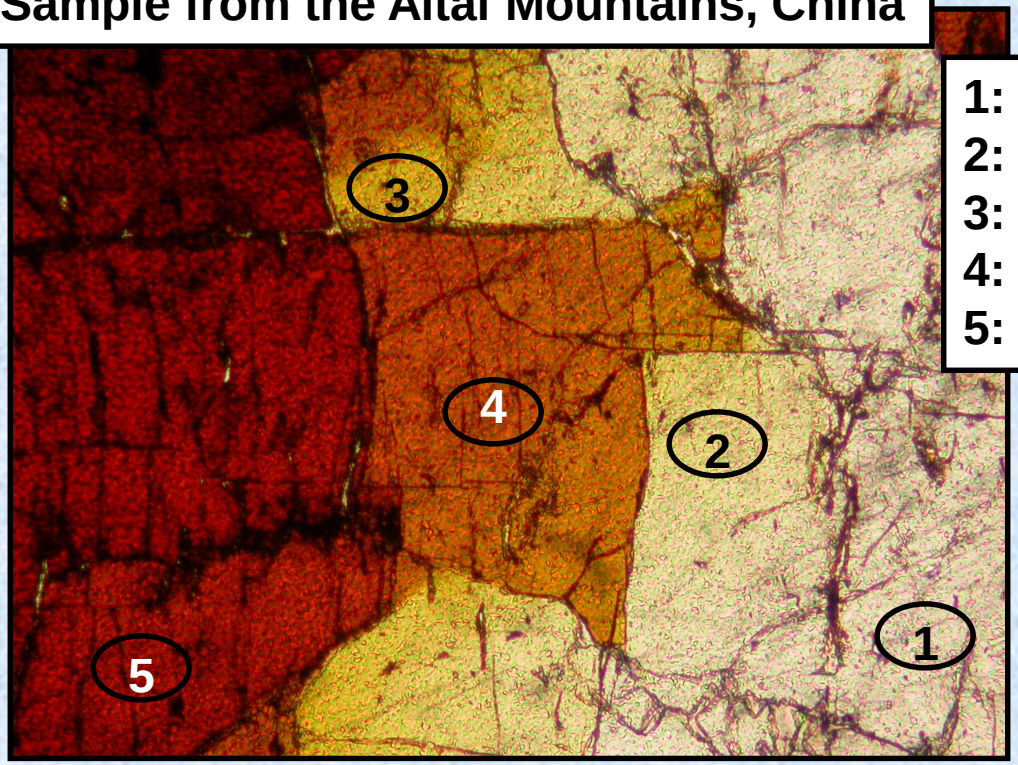

1: $Li_{0.93}(Fe^{2+}_{0.03}Fe^{3+}_{0.13}Mn^{2+}_{0.80})(PO_4)$
2: $Li_{0.96}(Fe^{2+}_{0.08}Fe^{3+}_{0.08}Mn^{2+}_{0.81})(PO_4)$
3: $Li_{0.88}(Fe^{3+}_{0.16}Mn^{2+}_{0.80}Mn^{3+}_{0.01})(PO_4)$
4: $Li_{0.82}(Fe^{3+}_{0.16}Mn^{2+}_{0.75}Mn^{3+}_{0.06})(PO_4)$
5: $Li_{0.69}(Fe^{3+}_{0.16}Mn^{2+}_{0.62}Mn^{3+}_{0.19})(PO_4)$

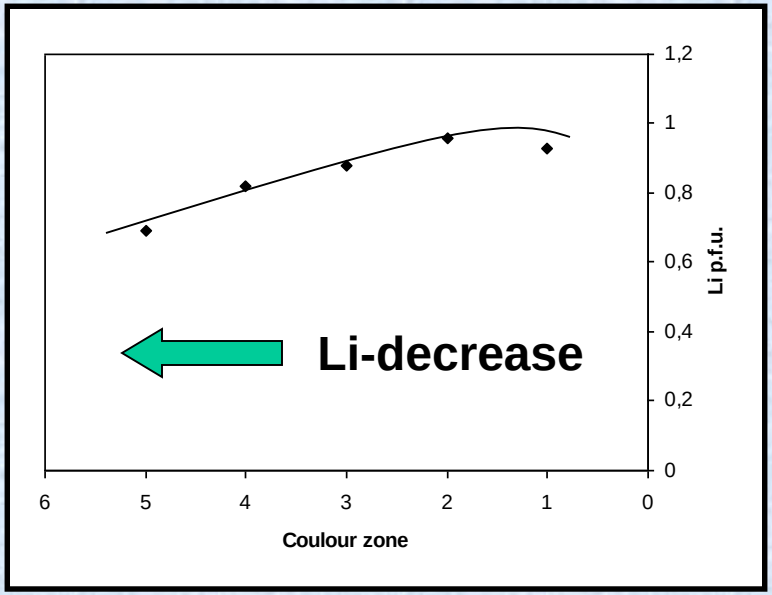

- The transition from lithiophilite to sicklerite is progressive
- The change in colour is due to the presence of Mn^{3+}

Variations of unit-cell parameters

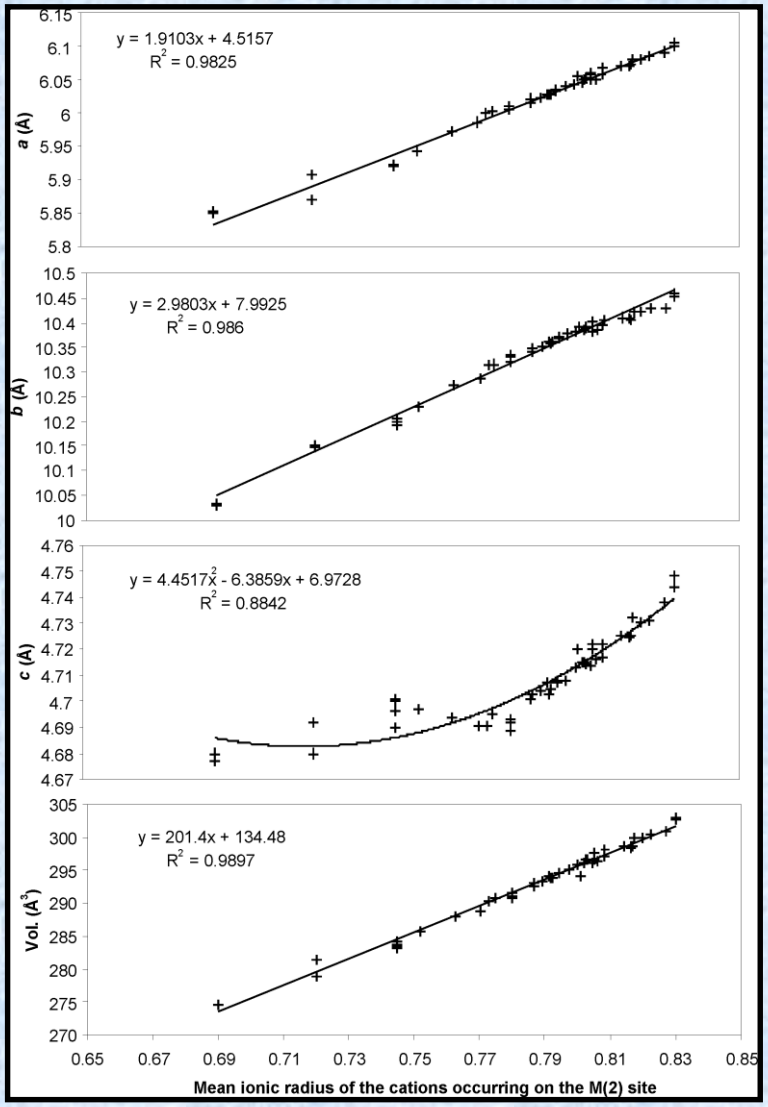

Good correlations

Accurate estimation of the Fe/Mn ratio of natural members of the triphylite-lithiophilite series, when the Mg content is lower than 0.016 *a.p.f.u.* (accuracy +/- 7 %)

Geological applications

Université de Liège

OBSERVATIONS:

•Primary assemblages involving alluaudite (alluaudite + fillowite, alluaudite + triphylite, alluaudite + arrojadite) were observed in pegmatites by Fransolet et al. (1994, 1997, 1998, 2004)

• Sarcopside and triphylite frequently show exsolution textures

QUESTIONS:

• Is it possible to reproduce these assemblages in the laboratory, by hydrothermal techniques?

• Which are the stability fields of these minerals and/or assemblages?

• Is it possible to obtain accurate data on the P/T/fO_2 conditions that prevailed in pegmatites, from these assemblages?

Stability of Fe-Mn phosphates

Université de Liège

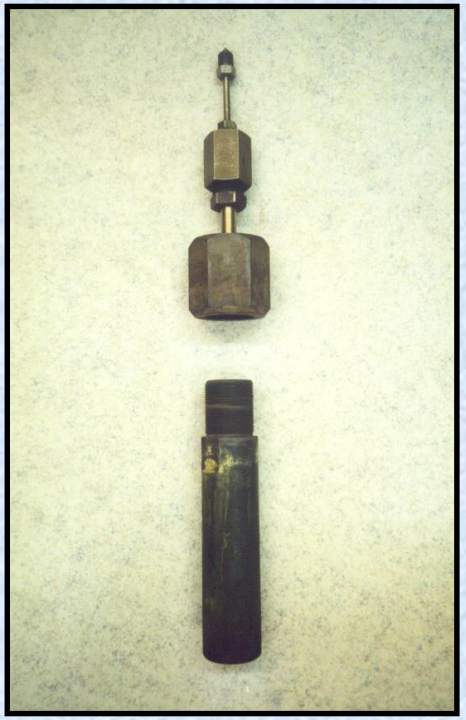

- Hydrothermal synthesis
- Tuttle-type cold-seal bombs
- T = 400-800 °C
- P = 1 kbar
- Double capsule method (Au 4 mm, $Ag_{70}Pd_{30}$ 2 mm)
- Oxygen fugacity: Ni/NiO (NNO) buffer

Université de Liège

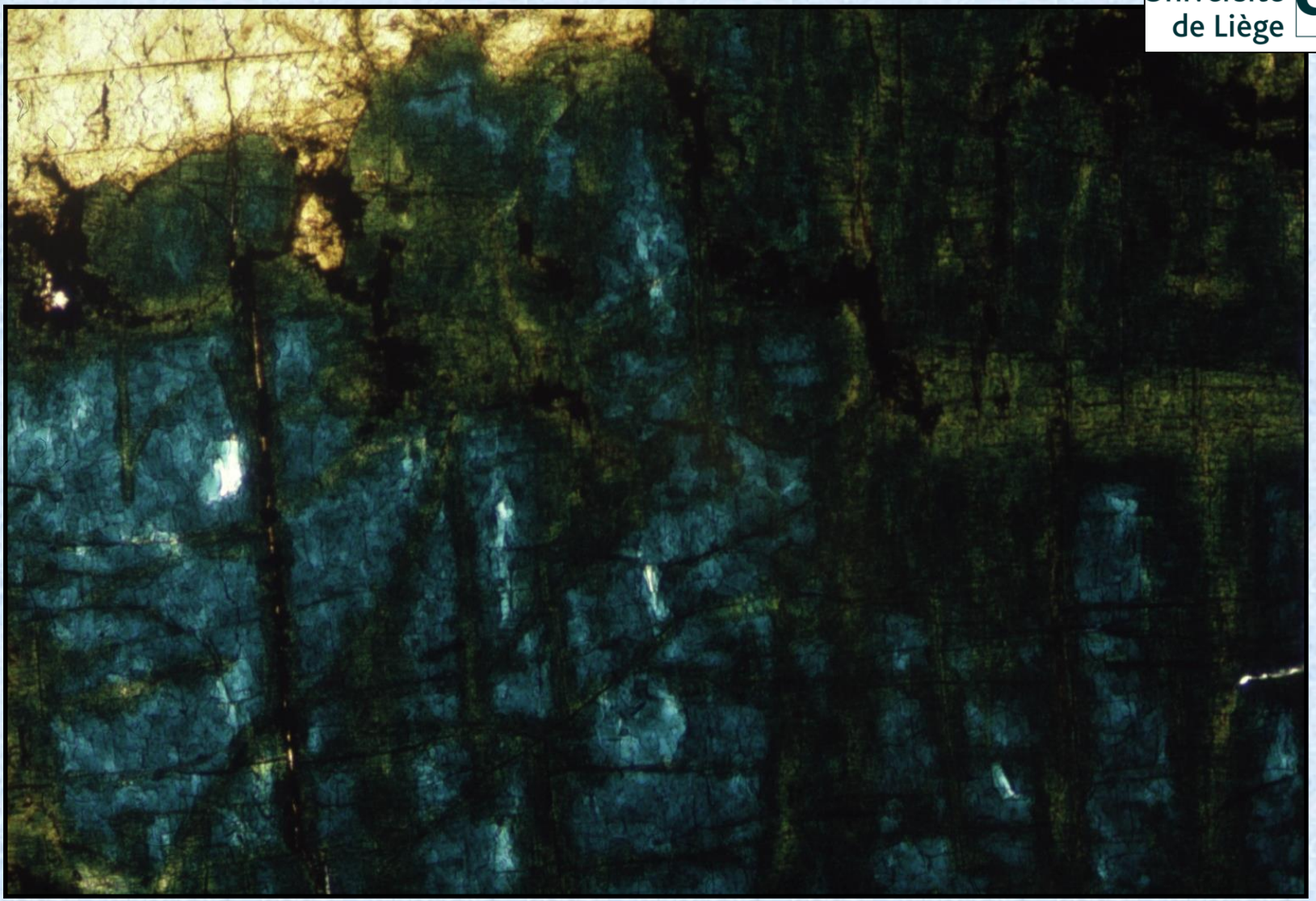

Ferroalluaudite, $NaFe^{2+}Fe^{3+}_2(PO_4)_3$, Angarf-sud, Morocco

A. The Na-Fe^{2+}-Fe^{3+} (+ PO_4) system

Université de Liège

★ = Ferroalluaudite from Angarf-sud, Morocco

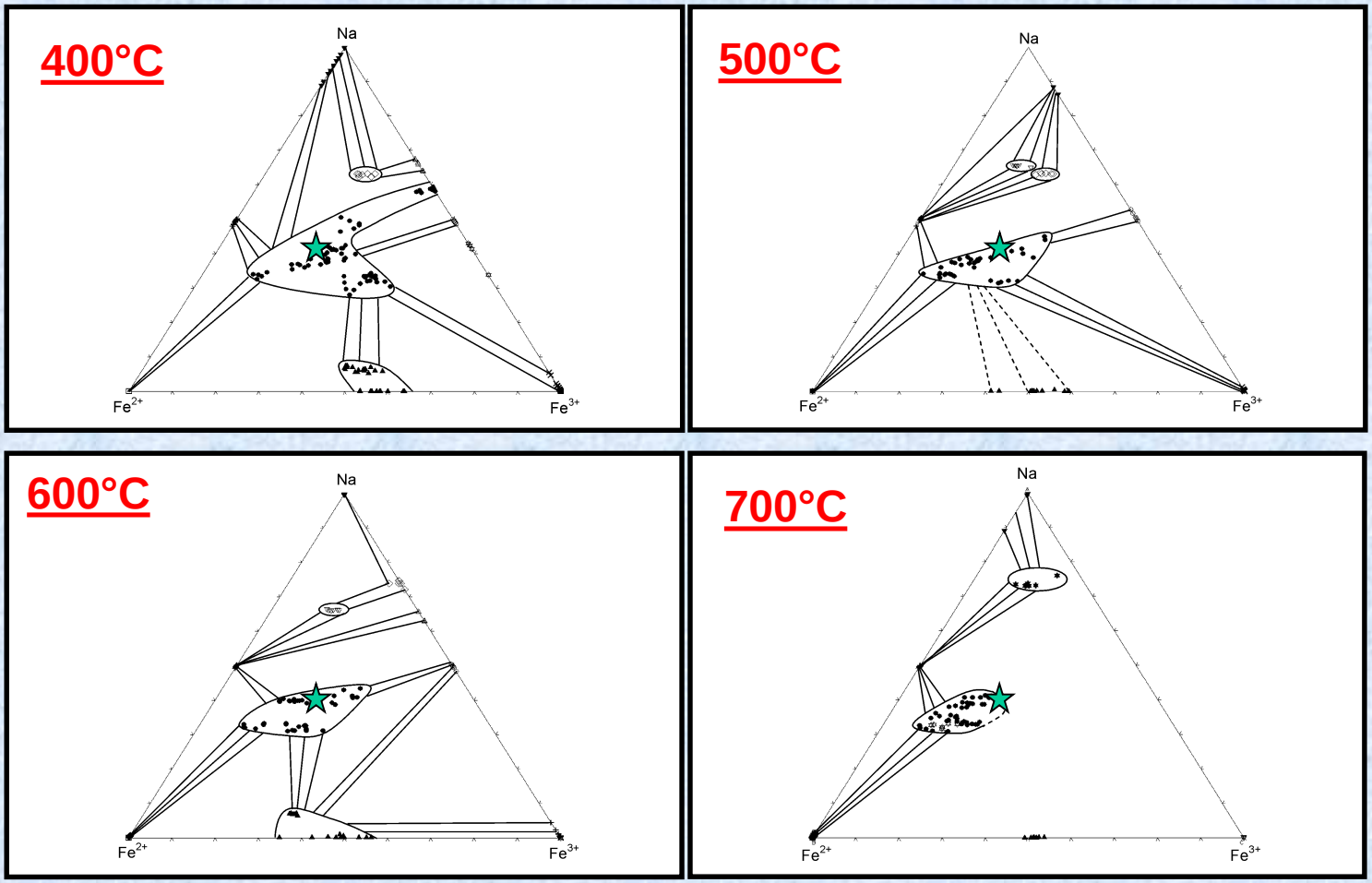

Cristallisation between 400 and 600°C → primary origin

B. The $Na_2(Mn_{1-x}Fe^{2+}_x)_2Fe^{3+}(PO_4)_3$ solid solution

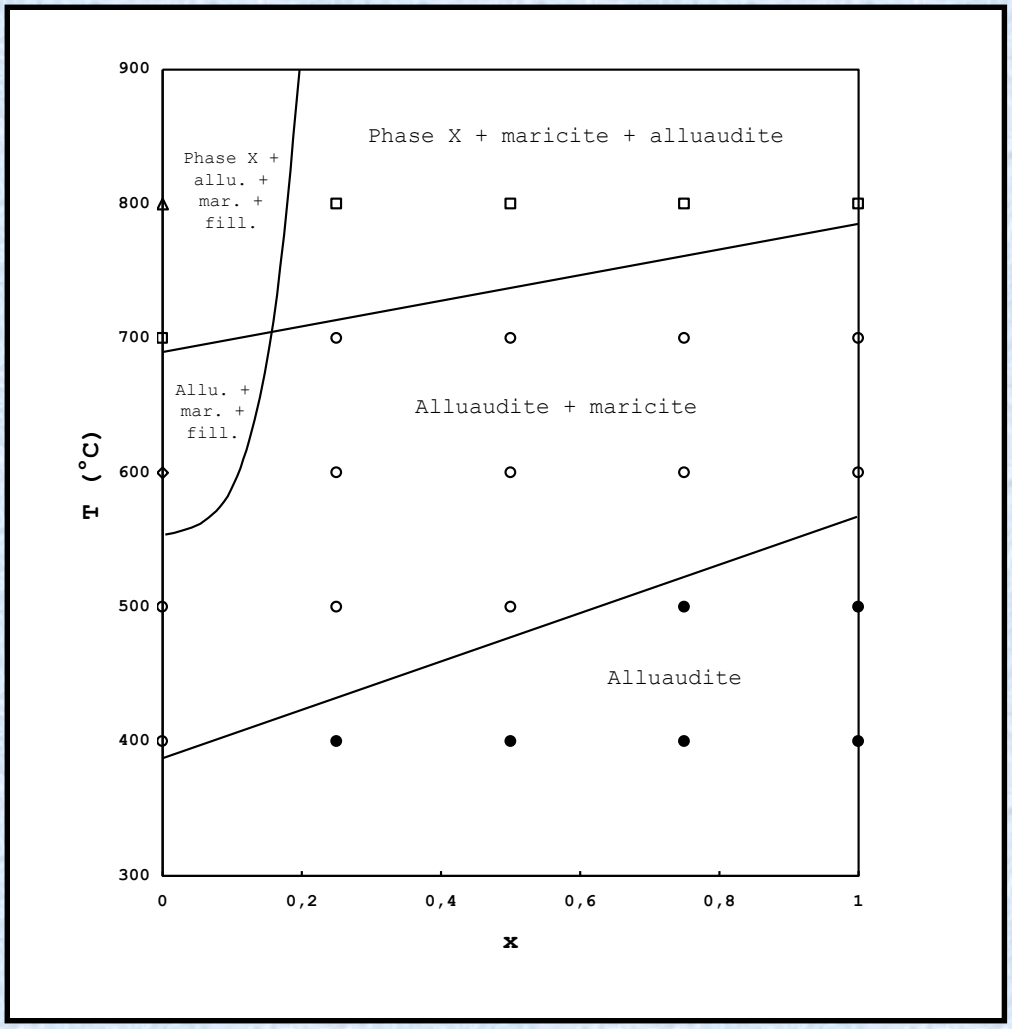

- **Low T** ⇒ alluaudite
- **High T** ⇒ "X-phase"
- **Mn** ⇒ fillowite [$NaMn_4(PO_4)_3$]

No maricite [$NaFePO_4$] in pegmatites

Varulite
$Na_2Mn_2Fe^{3+}(PO_4)_3$
350-400°C

Hagendorfite
$Na_2MnFe^{2+}Fe^{3+}(PO_4)_3$
450-500°C

Ferrohagendorfite
$Na_2Fe^{2+}{}_2Fe^{3+}(PO_4)_3$
550-600°C

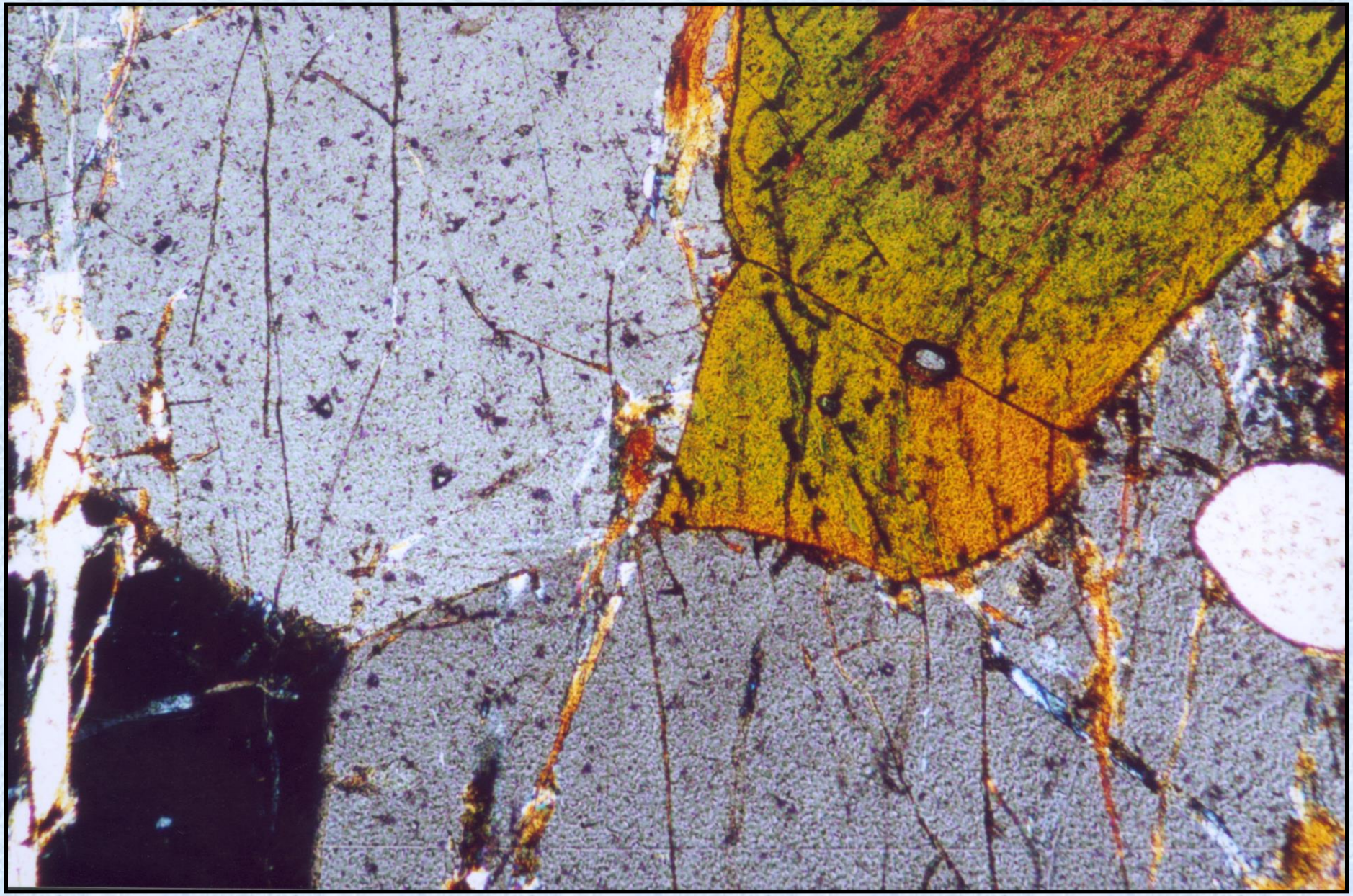

Alluaudite + fillowite, Kabira, Uganda

C. $Na_2MnFe^{2+}Fe^{3+}(PO_4)_3$

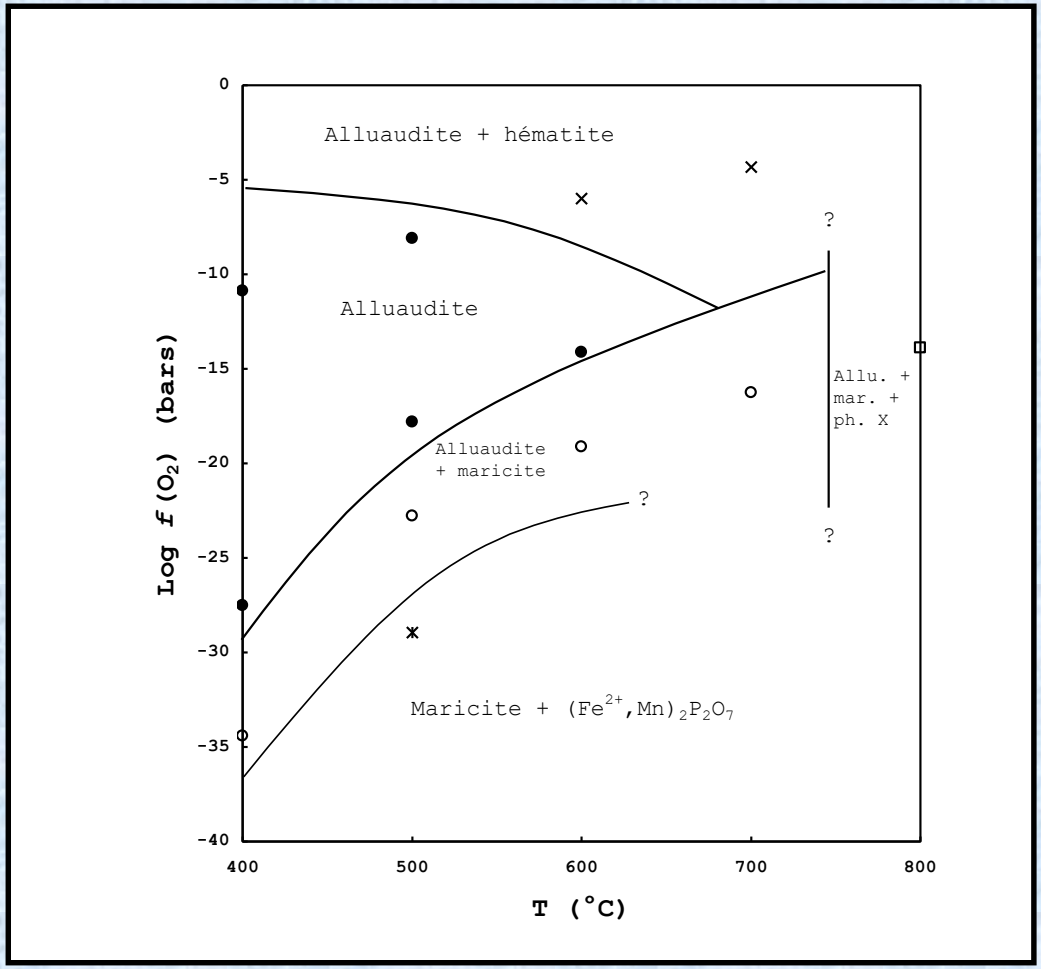

Composition of primary alluaudite

Temperature and oxygen fugacity can be constrained

D. The triphylite + alluaudite assemblage

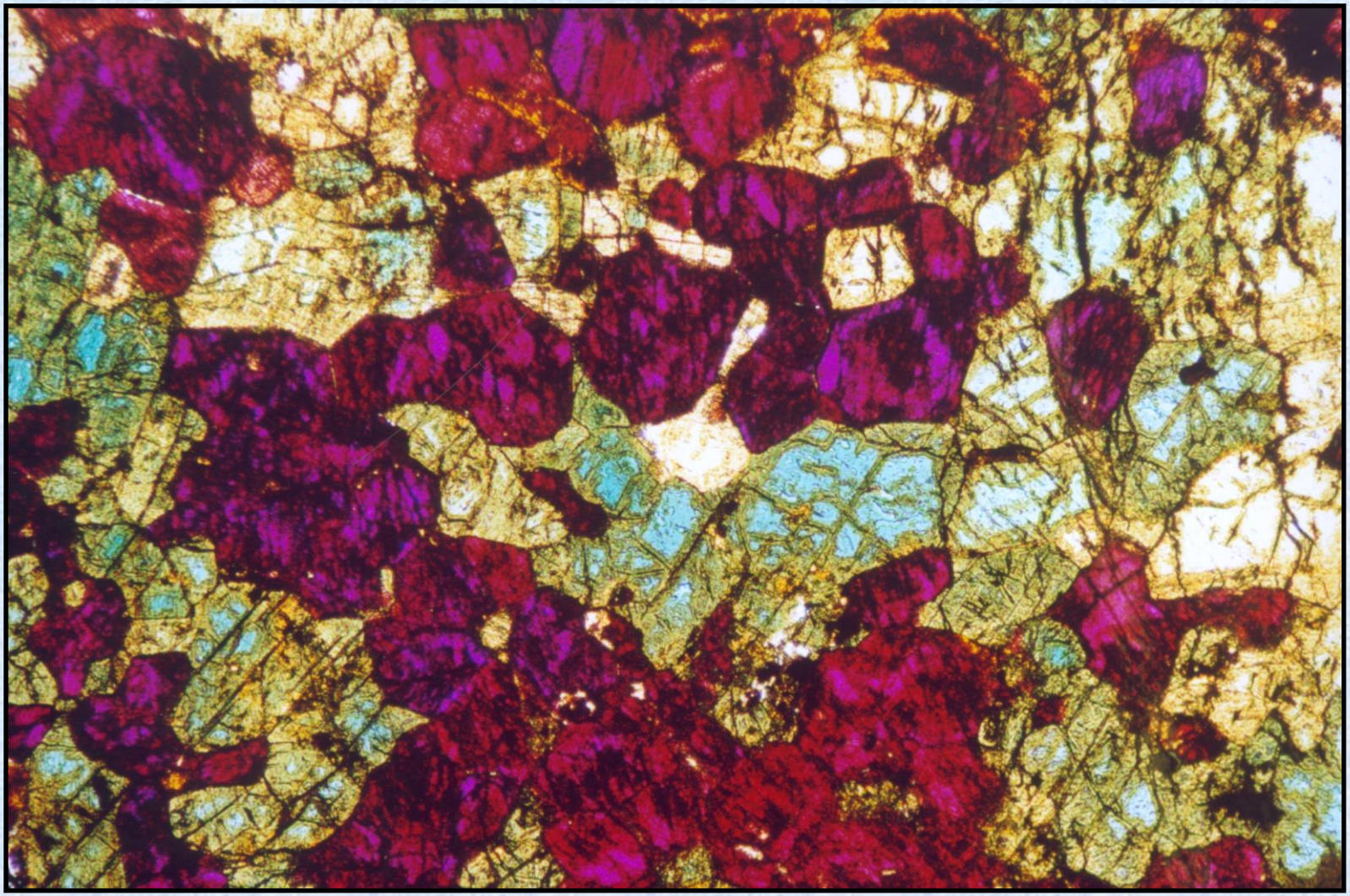

Hagendorfite, alluaudite, and heterosite, Kibingo pegmatite, Rwanda

Stability of the triphylite + alluaudite asemblage

Université de Liège

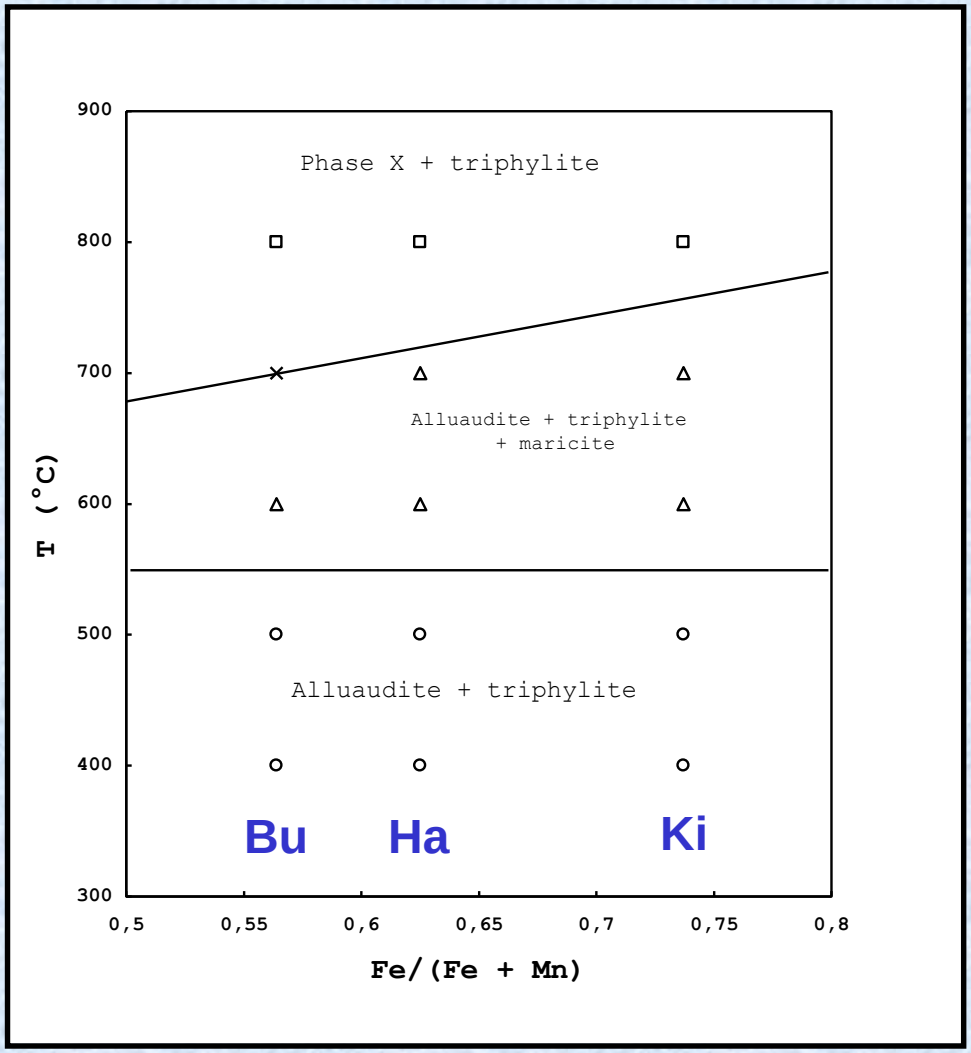

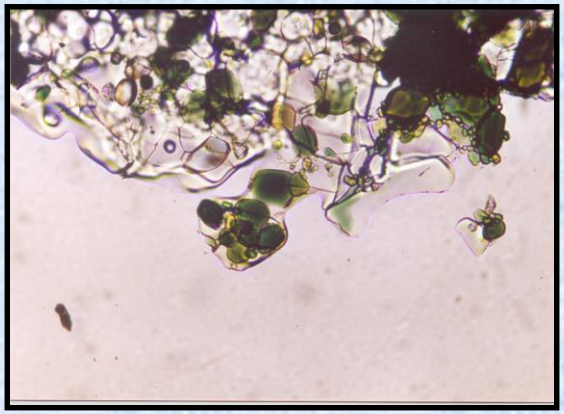

No maricite in pegmatites

Alluaudite + triphylite assemblage stable up to 500-600°C

Bu = Buranga, Rwanda
Ha = Hagendorf-Süd, Germany
Ki = Kibingo, Rwanda

The Na-in-triphylite geothermometer

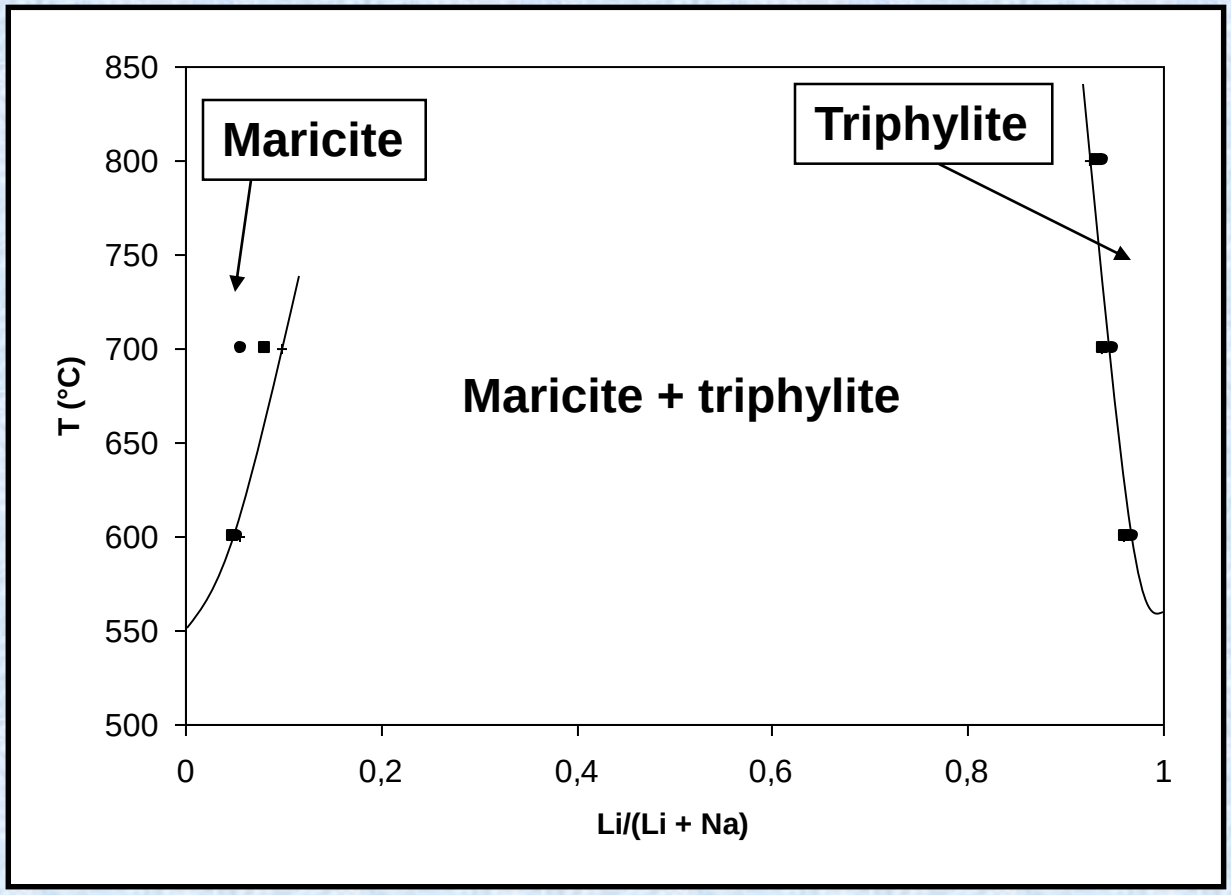

- **In triphylite, Na can reach 0.08 *a.p.u.f.* at 800°C**
- **In maricite, Li can reach 0.10 *a.p.u.f.* at 700°C**
- **No partitioning below ca. 550°C**

Geothermometer!

E. The triphylite + sarcopside assemblage

Université de Liège

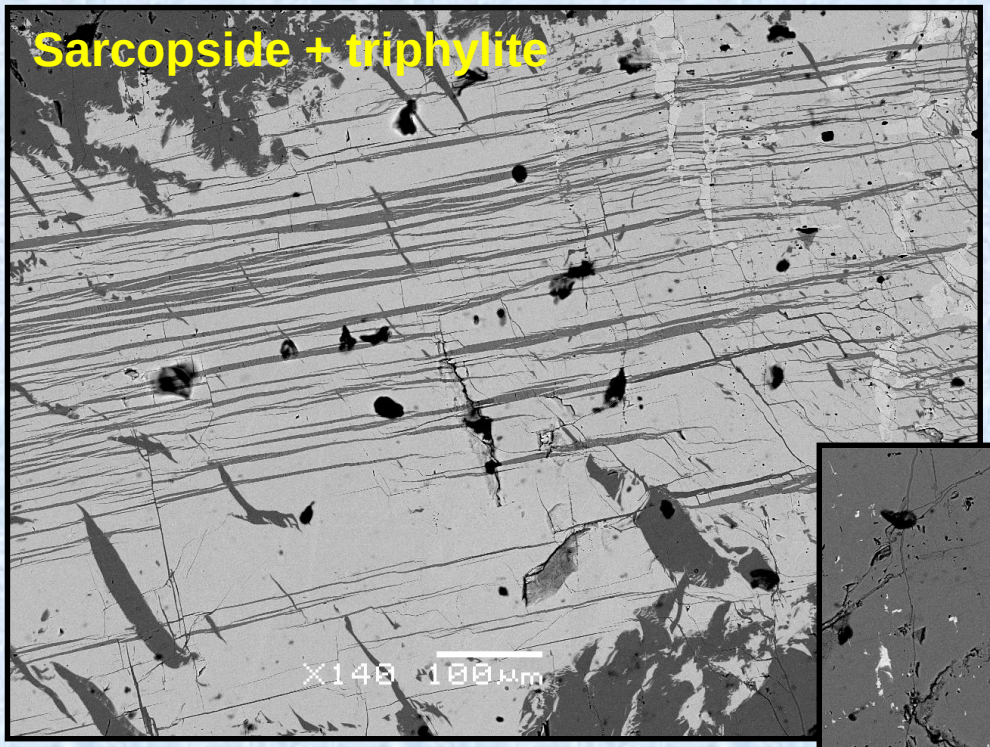

Cañada pegmatite, Spain

Lamellar textures

EXSOLUTIONS!!

Sarcopside $(Fe,Mn)_3(PO_4)_2$

Pictures: E. Roda Robles

Stability of the triphylite + sarcopside assemblage

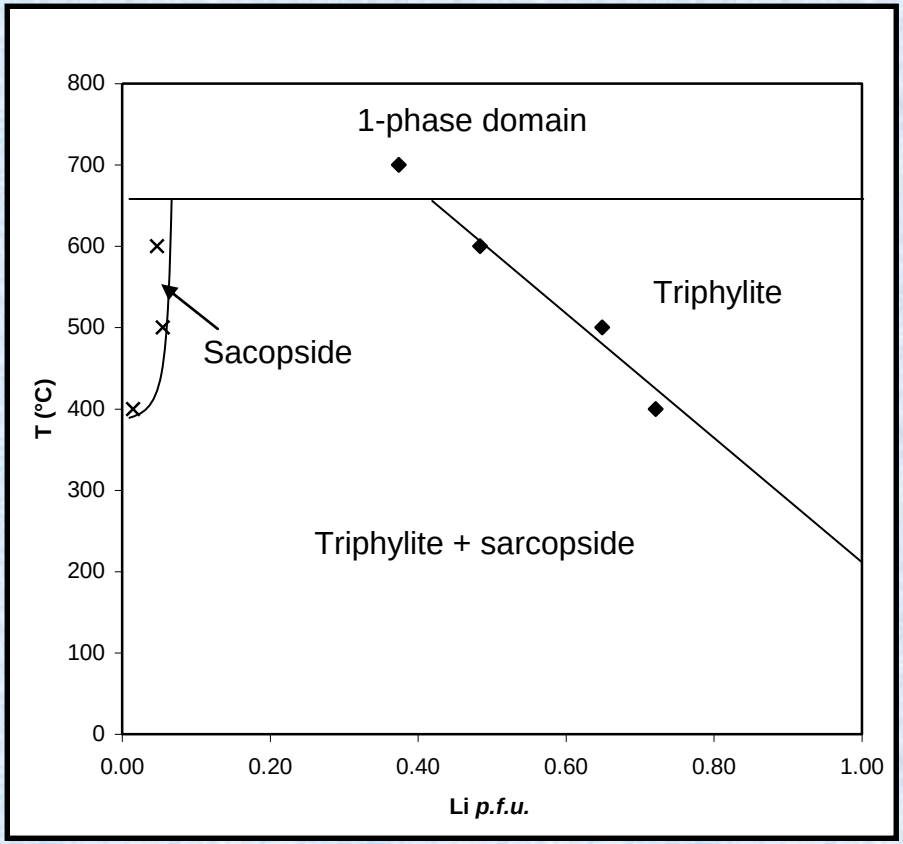

$LiFe^{2+}_{2.5}(PO_4)_2$

- **Decrease of the Li-content of triphylite, from 0.72 *a.p.f.u.* at 400°C, to 0.48 *a.p.f.u.* at 600°C**
- **Increase of the Li-content of sarcopside, from 0.01 *a.p.f.u.* at 400°C, to 0.05 *a.p.f.u.* at 600°C**
- **1-phase domain above 650°C**

Triphylite-sarcopside phase diagrams

Université de Liège

$LiMn_{0.5}Fe^{2+}_{2}(PO_4)_2$

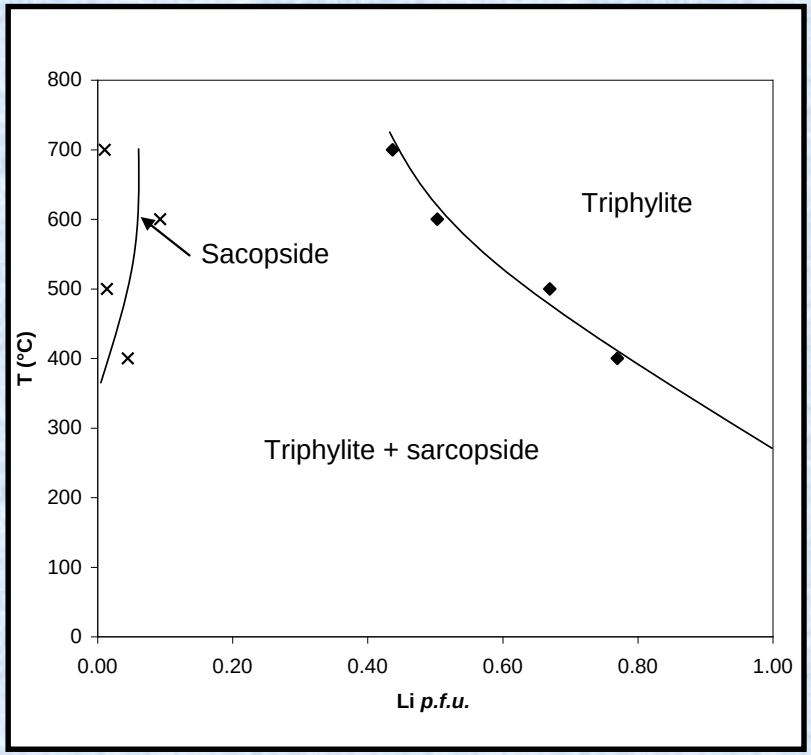

$LiMnFe^{2+}_{1.5}(PO_4)_2$

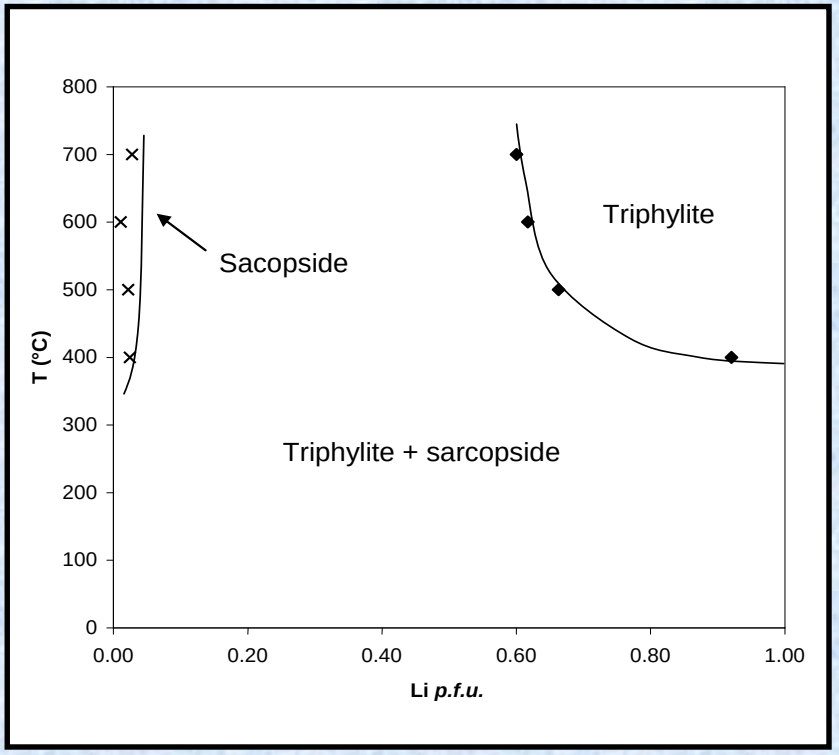

The Li-content of triphylite decreases with temperature

Geothermometer!

Calculation of crystallisation temperatures for natural assemblages

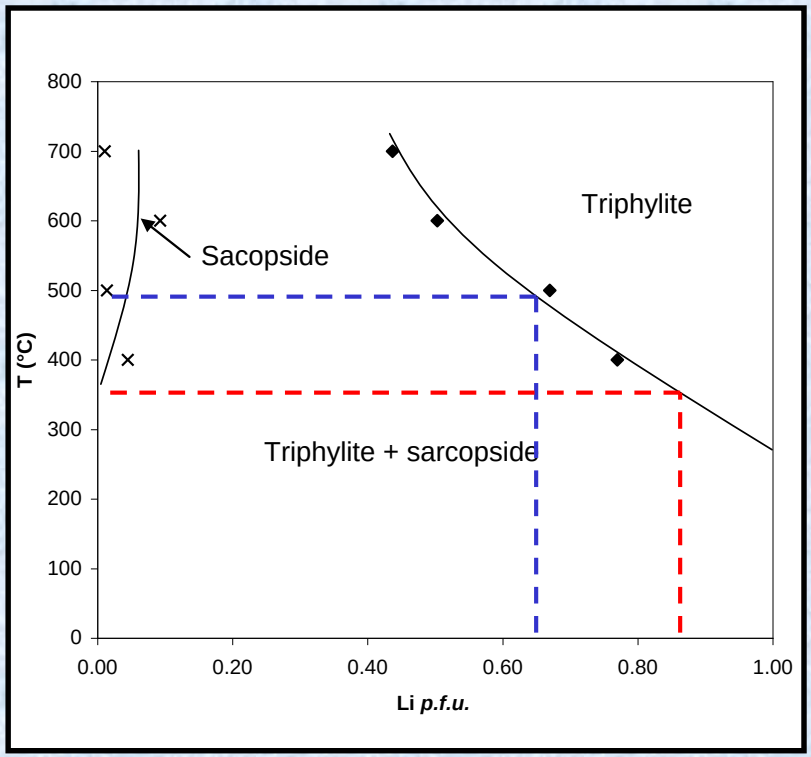

Fe/(Fe+Mn) ratio of natural triphylites and sarcopsides close to 0.800

Phase diagram for the $LiMn_{0.5}Fe^{2+}_2(PO_4)_3$ starting composition

Cañada

35 % sarcopside and 65 % triphylite

T ~ 500°C

Tsoabismund

15 % sarcopside and 85 % triphylite

T ~ 350°C

A. Applications: Li-ion batteries

Université de Liège

	Layered struct.		Spinel	Triphylite
	$LiCoO_2$	$LiNiCoO_2$	$LiMn_2O_4$	$LiFePO_4$
Capacity (mAh/g)	140-150	170-180	110-120	160-170
Potentiel (V)	3,9	3,8	4,0	3,4
Resistance to cycling	Poor	Poor	+/-	Good
Exchange speed	Good	Good	Good	Good
Electrode density	Good	+/-	+/-	Poor
Security	+/-	?	Good	Good
Cost of chemicals	High	+/-	Low	Low
Cost of synthesis	Low	High	+/-	Low
Abundance	Low	+/-	High	High
Toxicity	?	?	Low	Very low

Ref: N. Krins, Master thesis ULg, 2004 (LCIS)

$LiFe^{2+}(PO_4)$ as cathode material ?

Université de Liège

Electrochemical properties demonstrated by Padhi *et al*. (1997)

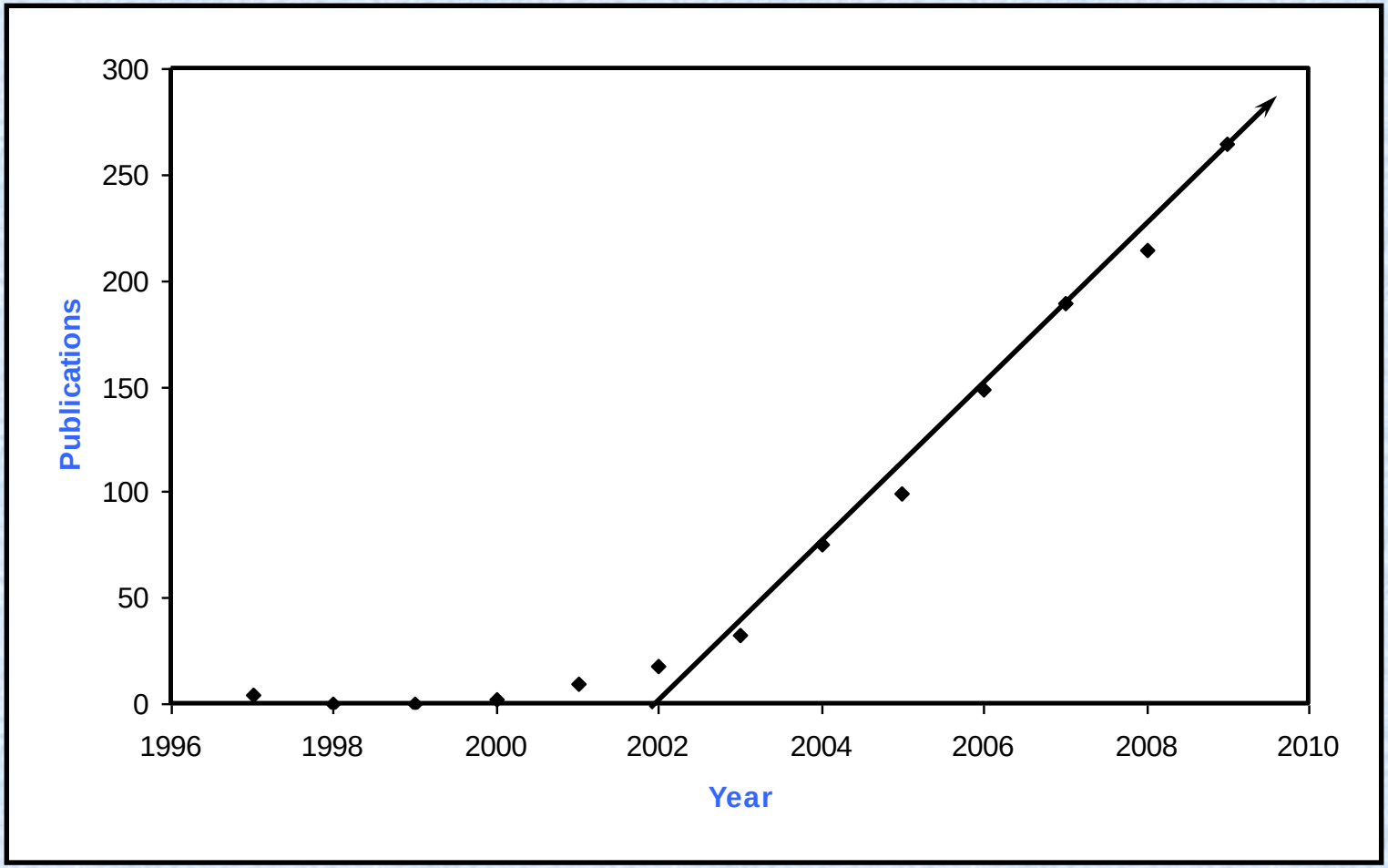

Ref: ISI web of knowledge – Current contents

Intercalation – extraction of Li

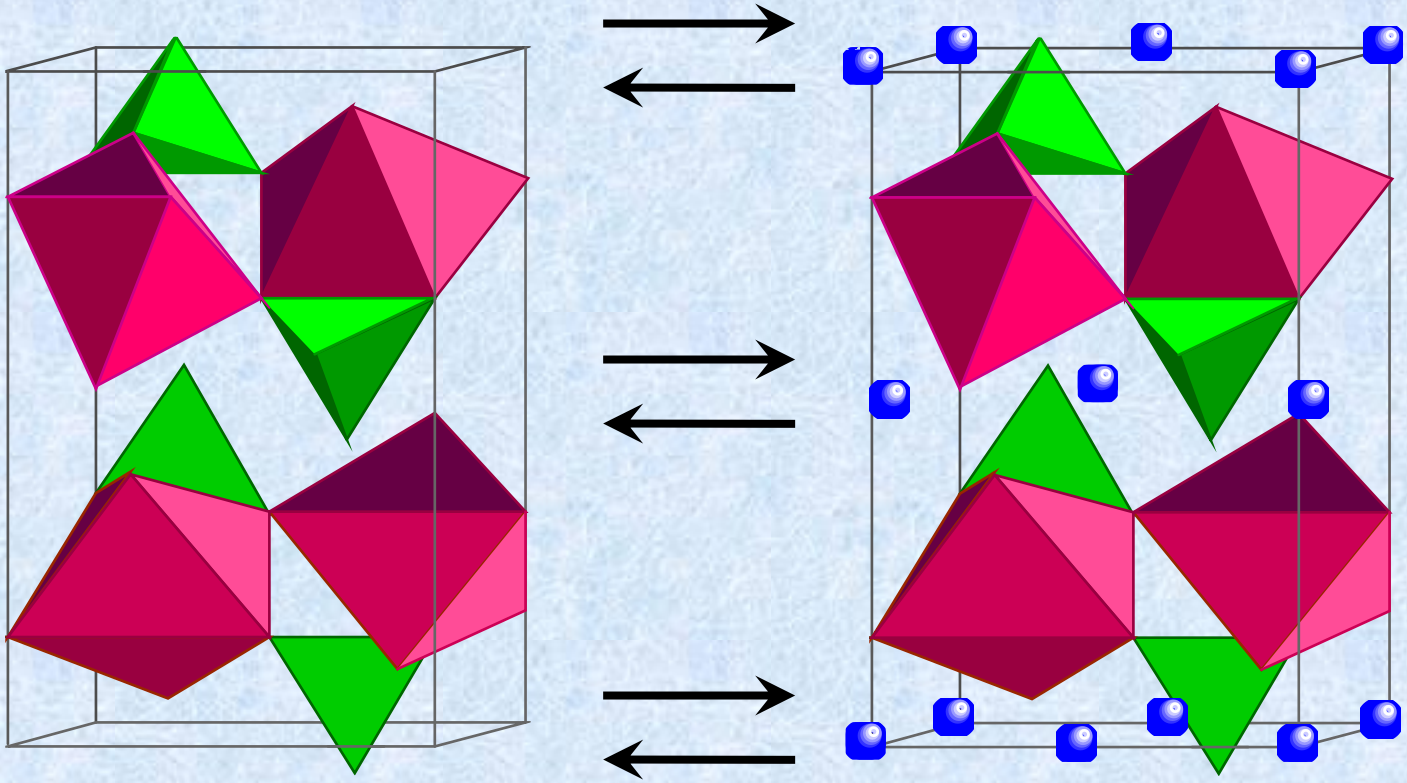

Heterosite, $Fe^{3+}(PO_4)$ **Triphylite, $LiFe^{2+}(PO_4)$**

Natural oxydation mechanism described by Quensel (1937) and Mason (1941)

Principle of Li-ion batteries

Université de Liège

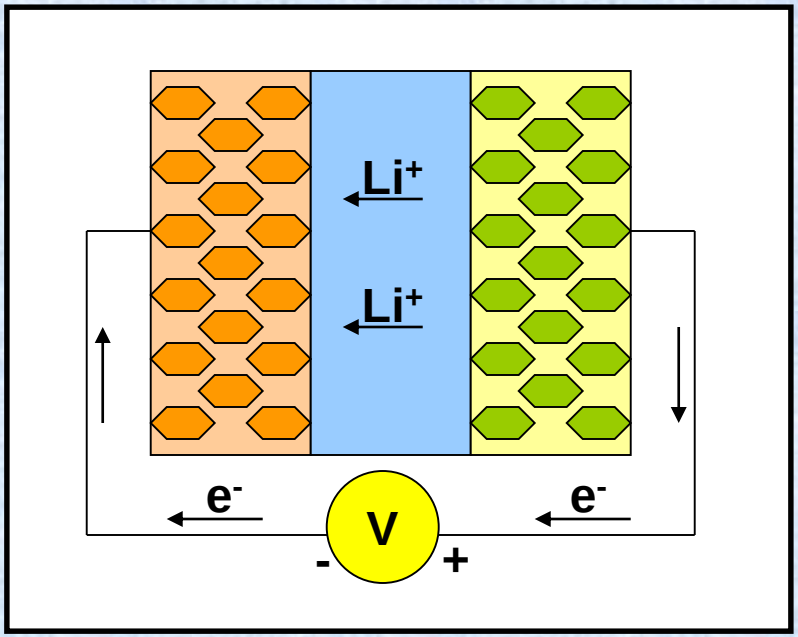

Charge

Discharge

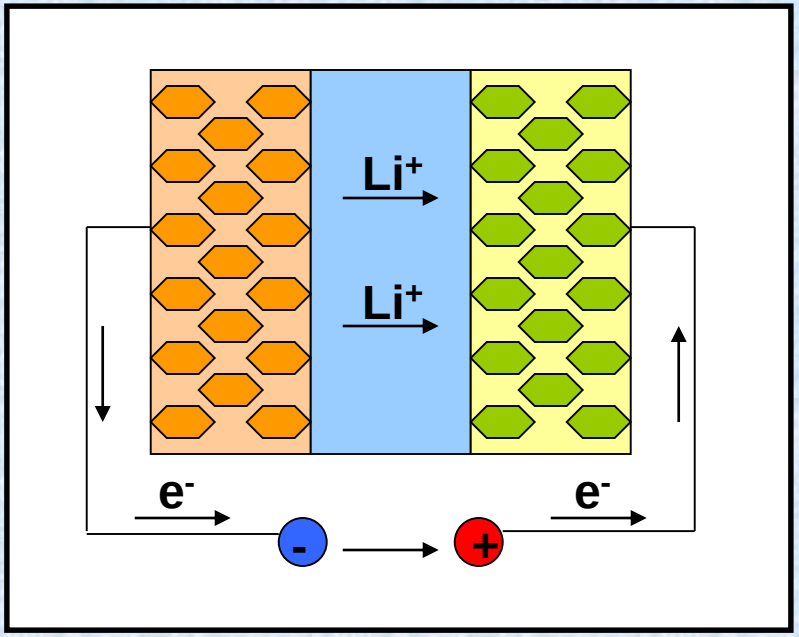

$LiFe^{2+}(PO_4)$ Metallic Li Electrolyte

Performance

Université de Liège

nature

Vol 458|12 March 2009|doi:10.1038/nature07853

LETTERS

Battery materials for ultrafast charging and discharging

Byoungwoo Kang[1] & Gerbrand Ceder[1]

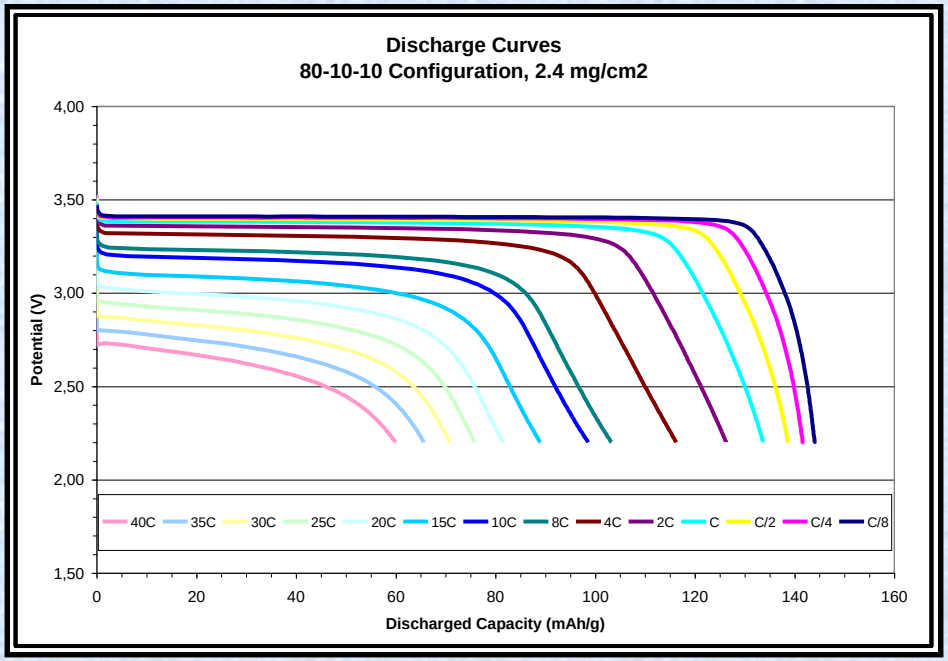

The storage of electrical energy at high charge and discharge rate is an important technology in today's society, and can enable hybrid and plug-in hybrid electric vehicles and provide back-up for wind and solar energy. It is typically believed that in electrochemical systems very high power rates can only be achieved with super-capacitors, which trade high power for low energy density as they only store energy by surface adsorption reactions of charged species on an electrode material[1–3]. Here we show that batteries[4,5] which obtain high energy density by storing charge in the bulk of a material can also achieve ultrahigh discharge rates, comparable to those of supercapacitors. We realize this in $LiFePO_4$ (ref. 6), a material with high lithium bulk mobility[7,8], by creating a fast ion-conducting surface phase through controlled off-stoichiometry. A rate capability equivalent to full battery discharge in 10–20 s can be achieved.

$LiFePO_4$-based batteries production

- Phostech Lithium was founded in 2001
- Based on the commercial potential of C-$LiFePO_4$ and other Phosphate-based cathode materials
- Obtained exclusive rights for the manufacture and sales of $LiFePO_4$ for Lithium-Ion battery applications with University of Texas and Hydro-Quebec
- Obtained through UDM the access to four improvement patents resulting from UDM's research for Hydro-Québec, including C additive to $LiFePO_4$ and a new synthesis way from a Fe^{+3} precursor

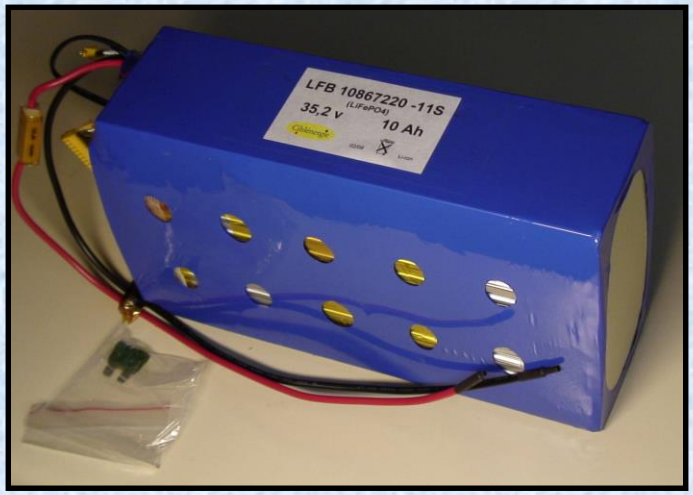

Université de Liège

$LiFePO_4$-based batteries applications

- **Cars**
- **Bicylces**
- **Motorbikes**
- **Mobile phones**
- **Laptops**
- **Storage of green energy**

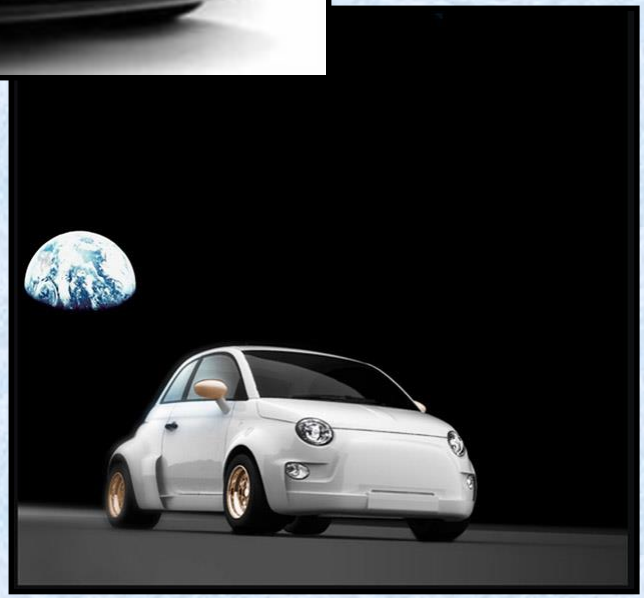

B. Applications: catalytic properties

Université de Liège

Probe reaction: Butan-2-ol ⇒ Methyl ethyl ketone + butenes + CO_2

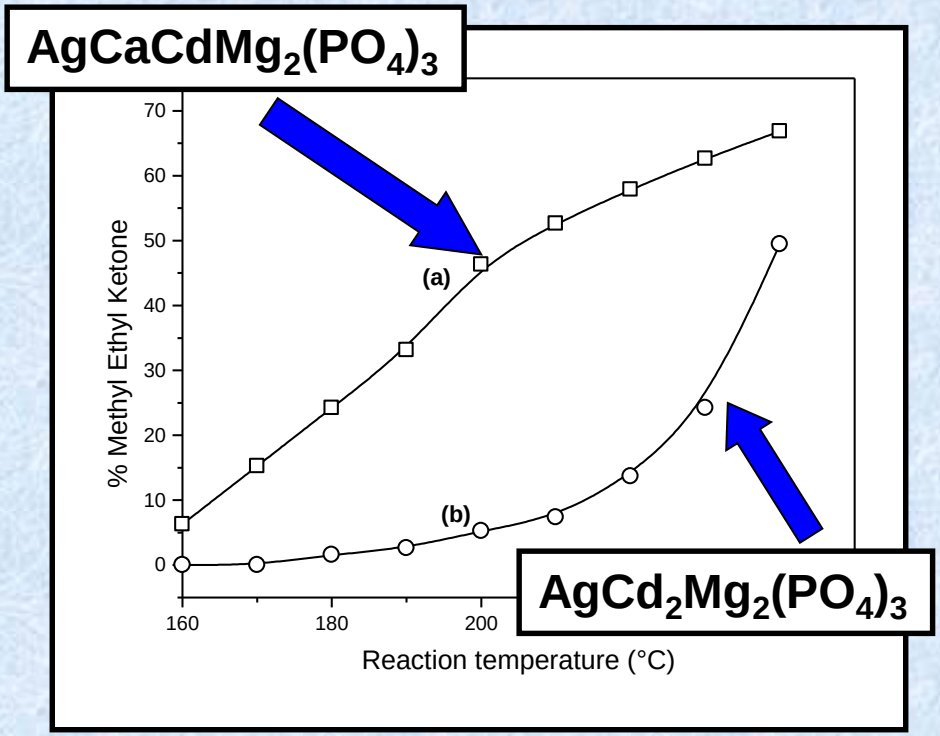

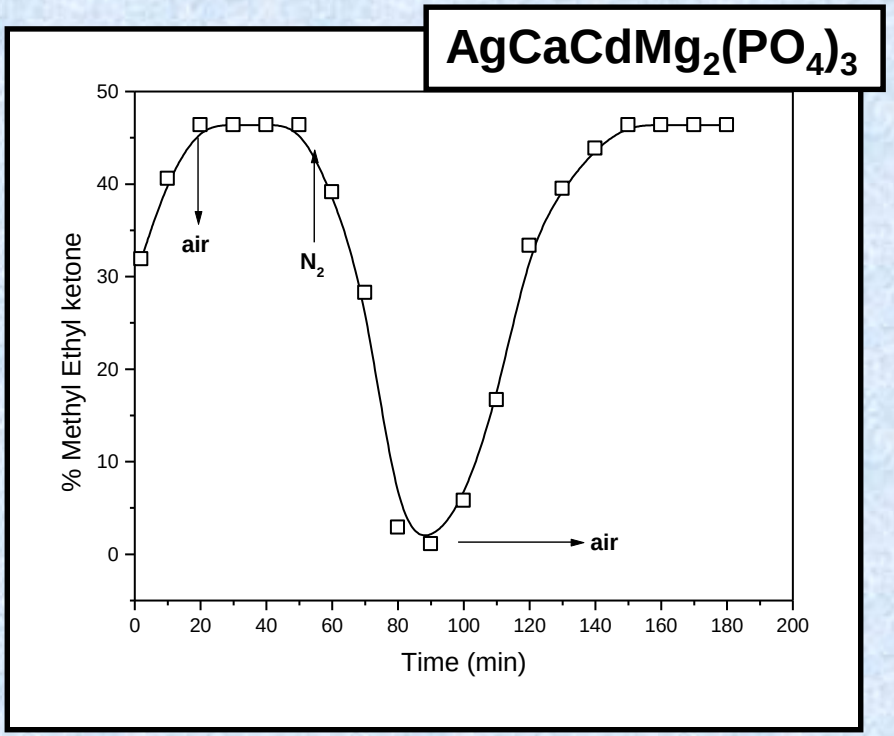

⇒ Catalytic activity comparable to that of nasicon-type phosphates

Kacimi *et al*. (2005), Materials Research Bulletin

Alluaudites as a promizing cathode material for Li-ion batteries?

Université de Liège

$Li_xNa_{2-x}Mn_2Fe^{3+}(PO_4)_3$

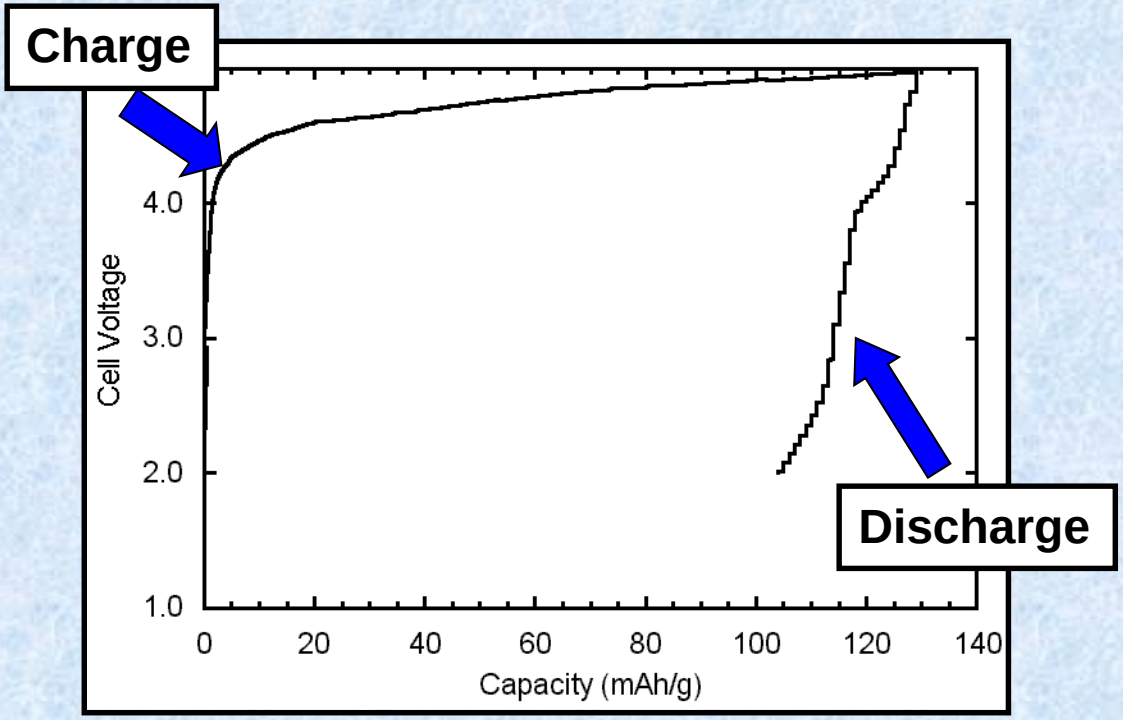

Low performance

Investigation of other alluaudite-type phosphates necessary

Richardson (2003), J. Power Sources, 119-121, 262-265

Conclusions

- Iron-manganese phosphates play a crucial role in the geochemical evolution of granitic pegmatites, and are very sensitive to the variations of physico-chemical parameters

- An experimental investigation of alluaudites, and of the alluaudite + triphylite and triphylite + sarcopside assemblages, has provided tools which can be used to estimate the P, T, and oxygen fugacity conditions that prevailed in pegmatites

- Phosphates with the olivine- and alluaudite-type structures show interesting properties, related to the mobility of large cations in their crystal structures. These properties are responsible for the recent use of $LiFePO_4$ as electrode material in Li-ion batteries.